Available online at www.sciencedirect.com

SCIENCE DIRECT®

International Journal of Solids and Structures 43 (2006) 2646–2669

INTERNATIONAL JOURNAL OF SOLIDS and STRUCTURES

www.elsevier.com/locate/ijsolstr

Robustness analysis of trusses with separable load and structural uncertainties

Y. Kanno *, I. Takewaki

Department of Urban and Environmental Engineering, Kyoto University, Kyoto 606-8501, Japan

Received 20 January 2005; received in revised form 30 June 2005
Available online 30 August 2005

Abstract

This paper discusses evaluation techniques of the robustness function of trusses, which is regarded as one of measures of structural robustness, under the uncertainties of member stiffnesses and external forces. By using quadratic embedding of the uncertainty and the $\mathscr{S}$-procedure, we formulate a quasiconvex optimization problem which provides lower bounds of the robustness functions. A bisection method is proposed, where we solve a finite number of semidefinite programming problems in order to obtain a global optimal solution to the proposed quasiconvex optimization problem. The lower bounds of the robustness functions are computed for various trusses under several uncertainty circumstances.

Keywords: Robustness; Structural safety; Semidefinite program; Quasiconvex optimization; Data uncertainty

1. Introduction

In structural and mechanical design, deterministic design optimization models have been successfully developed. Recently, the robust structural design has received increasing attention, which may decrease the sensitivities of mechanical performance with respect to various uncertain parameters. For this purpose, a number of reliability-based optimization methods as well as the robust optimal design methods have been proposed (Ben-Tal and Nemirovski, 1997; Choi et al., 2001; Doltsinis and Kang, 2004; Kharmanda et al., 2004; Tsompanakis and Papadrakakis, 2004).

* Corresponding author. Tel./fax: +81 75 753 5778.
E-mail addresses: kanno@archi.kyoto-u.ac.jp (Y. Kanno), takewaki@archi.kyoto-u.ac.jp (I. Takewaki).

0020-7683/$ - see front matter
doi:10.1016/j.ijsolstr.2005.06.088

Based on stochastic uncertainty models of mechanical parameters, various techniques were proposed for evaluation and estimation of failure probability (Kharmanda et al., 2004; Tsompanakis and Papadrakakis, 2004), that can be utilized in the reliability-based structural design methods. Various formulations for sensitivity analysis of probabilistic structural performance were also proposed (Choi et al., 2001; Doltsinis and Kang, 2004).

Besides stochastic uncertainty models, non-probabilistic uncertainty models have also been developed, where so-called *unknown-but-bounded* uncertain parameters are included in a system. Ben-Haim and Elishakoff (1990) developed the so-called *convex model*, with which Pantelides and Ganzerli (1998) proposed a robust truss optimization method. For various classes of convex optimization problems, a unified methodology of *robust optimization*, or *robust counterpart* scheme, was developed by Ben-Tal and Nemirovski (2002), where the data in optimization problems are assumed to be unknown but bounded. Calafiore and El Ghaoui (2004) proposed a method for finding the ellipsoidal bounds of the solution set of uncertain linear equations by using the semidefinite program. Ben-Tal and Nemirovski (1997) solved the minimization problem of compliance of a truss under unknown-but-bounded external forces.

Recently, as a measure of robustness of mechanical systems, Ben-Haim (2001) proposed the concept of *robustness function*, which expresses the greatest level of non-probabilistic uncertainty at which any constraint on mechanical performance cannot be violated. The robustness function has an advantage, compared with the reliability analyses based on stochastic uncertainty models, such that engineers have to estimate neither the level of uncertainty nor the probabilistic distribution of uncertain parameters, which are often difficult to estimate in practical situations.

In many practical problems, it is difficult to compute the robustness functions, which has prevented us from applying the robustness function to the robust mechanical design. Indeed, in order to compute the robustness function for general cases, we have to solve an optimization problem with infinitely many constraint conditions. See, for more details, Section 3.3. Hence, it is strongly desired to develop an efficient method for computing the robustness functions of trusses. Under the assumption that only the external forces possess uncertainty, the authors proposed computable formulations of the robustness functions of trusses (Kanno and Takewaki, 2004a). Takewaki and Ben-Haim (in press) computed the robustness functions in a particular case where the most critical case can be obtained analytically. However, to the authors' knowledge, no efficient method has ever been proposed which enables us to evaluate the robustness functions when the stiffness matrix of a truss also includes uncertain parameters.

In this paper, we deal with a linear elastic truss subjected to uncertainties of external forces and stiffness of members. Particularly, we pay much attention to the case where the truss can be modeled as combination of two trusses, which have different characteristics of uncertainty. Consider the following two trusses:

(i) a truss with the certain member stiffness supporting the uncertain external forces;
(ii) a truss consisting of members with uncertain stiffness under the certain external forces.

The member locations of these trusses are assumed to be certain. Small rotations and small strains are assumed. We say that a truss obeys *separable uncertainty* model if the truss is modeled as a combination of trusses (i) and (ii). By *separable* we mean that a structure can be divided into the two components (i) and (ii), where the truss (i) possesses uncertain parameters only in the external forces, and the truss (ii) includes uncertain parameters only in the member stiffnesses.

In many practical situations, e.g., structure–soil interaction models, we can divide a structural system into two parts, one of which principally suffers the uncertain external loads, and the other has relatively large uncertainties of the stiffness parameters. In such cases, the separable uncertainty models of trusses can be used as approximation models of the uncertainty structural systems. In the case of a structure–soil interaction model, the stiffness parameters of the structure are relatively certain, whereas the soil has very large uncertainties of the stiffness parameters. It is obvious that the separable uncertainty model includes a structure consisting of either the truss (i) or (ii).

Our purpose is to propose an efficient algorithm for computing the robustness functions of trusses with separable uncertainties. Particularly, we formulate a numerically tractable optimization problem, which provides a lower bound on the robustness function. Note that a lower bound is regarded as a conservative estimation of the robustness function, i.e., a level of uncertainty at which the satisfaction of the constraints of mechanical performance is guaranteed. Hence, finding a lower bound, not an upper bound, is meaningful when it is difficult to find the exact value of the robustness function.

Our approach in this paper is summarized as follows. We first show that the robustness function can be obtained as the optimal objective value of an optimization problem with a finite number of variables and infinitely many constraint conditions. Secondly, by using quadratic embedding of the uncertainty and the $\mathscr{S}$-procedure (Ben-Tal and Nemirovski, 2001, Section 4.10.5), we formulate a finite-dimensional optimization problem that provides a lower bound on the robustness function. This fundamental idea is similar to that used in Calafiore and El Ghaoui (2004). The obtained problem is shown to be a quasiconvex optimization problem. Finally, we propose a bisection algorithm based on a convex feasibility problem (Boyd and Vandenberghe, 2004, Section 4.2.5), which finds a global optimal solution of the proposed problem by solving a finite number of the *semidefinite programming* (SDP) problems (Wolkowicz et al., 2000). At each iteration of the algorithm, an SDP problem can be efficiently solved by using the primal–dual interior-point method (Kojima et al., 1997).

It should be emphasized that this approach can be extended to a more general representation of uncertainty models. Indeed, as shown in Section 4, the assumption of separable uncertainty is not necessarily to constructing a quasiconvex optimization problem providing a lower bound on the robustness function. In this context, we shall observe that the separable uncertainty is regarded as a special case where the size of problems solved in our algorithm size can be reduced. See, for more details, Remarks 4.5 and 4.7.

This paper is organized as follows. In Section 2, in order to make this paper self-contained, we introduce SDP and quasiconvex optimization problems, as well as some useful technical results. Section 3 introduces a separable uncertainty model of trusses. We formulate in Section 3.3, an optimization problem with infinitely many constraints such that the optimal objective value coincides with the robustness function of trusses. Section 4 presents a quasiconvex optimization problem with a finite number of variables and constraints in order to compute a lower bound on the robustness function. We also propose an algorithm, which finds a global optimal solution of the present quasiconvex optimization problem. Numerical experiments are presented in Section 5 for trusses under various uncertainty circumstances. We conclude the paper in Section 6.

2. Preliminary results

In this paper, all vectors are assumed to be column vectors. However, for vectors $\boldsymbol{p} \in \mathbf{R}^m$ and $\boldsymbol{q} \in \mathbf{R}^n$, we often simplify the notation $(\boldsymbol{p}^\top, \boldsymbol{q}^\top)^\top$ as $(\boldsymbol{p}, \boldsymbol{q})$. For two sets $U \subseteq \mathbf{R}^m$ and $V \subseteq \mathbf{R}^n$, their Cartesian product is defined by $U \times V = \{(\boldsymbol{u}, \boldsymbol{v}) \in \mathbf{R}^{m+n} \,|\, \boldsymbol{u} \in U, \boldsymbol{v} \in V\}$. Particularly, we write $\mathbf{R}^{m+n} = \mathbf{R}^m \times \mathbf{R}^n$.

The standard Euclidean norm $\|\boldsymbol{p}\|_2 = (\boldsymbol{p}^\top \boldsymbol{p})^{1/2}$ of a vector $\boldsymbol{p} \in \mathbf{R}^n$ is often abbreviated by $\|\boldsymbol{p}\|$. $\|\boldsymbol{p}\|_\infty$ denotes the l_∞-norm of $\boldsymbol{p} = (p_i) \in \mathbf{R}^n$ defined as

$$\|\boldsymbol{p}\|_\infty = \max_{i \in \{1,\ldots,n\}} |p_i|.$$

Let $\mathbf{R}^n_+ \subset \mathbf{R}^n$ denote the non-negative orthant defined by

$$\mathbf{R}^n_+ = \{\boldsymbol{x} = (x_i) \in \mathbf{R}^n \mid x_i \geqslant 0, i = 1, \ldots, n\}.$$

For a set X, we denote by $\mathscr{P}(X)$ the power set of X.

2.1. Semidefinite program

Let $\mathcal{S}^n \subset \mathbf{R}^{n \times n}$ denote the set of all $n \times n$ real symmetric matrices. $\mathcal{S}^n_+ \subset \mathcal{S}^n$ denotes the set of all positive semidefinite matrices. We write $\boldsymbol{P} \succeq \boldsymbol{O}$ and $\boldsymbol{P} \succeq \boldsymbol{Q}$, respectively, if $\boldsymbol{P} \in \mathcal{S}^n_+$ and $\boldsymbol{P} - \boldsymbol{Q} \in \mathcal{S}^n_+$.

For any $\boldsymbol{P} \in \mathcal{S}^n$ and $\boldsymbol{Q} \in \mathcal{S}^n$, we designate by $\boldsymbol{P} \bullet \boldsymbol{Q}$ the standard inner product of $\boldsymbol{P}$ and $\boldsymbol{Q}$ in the linear space $\mathcal{S}^n$, i.e.,

$$\boldsymbol{P} \bullet \boldsymbol{Q} = \mathrm{tr}(\boldsymbol{P}^\top \boldsymbol{Q}) = \sum_{i=1}^{n} \sum_{j=1}^{n} P_{ij} Q_{ij}.$$

The *semidefinite programming* (SDP) problem refers to the optimization problem having the form of (Wolkowicz et al., 2000)

$$\left.\begin{array}{ll} \min & \boldsymbol{C} \bullet \boldsymbol{X}, \\ \text{s.t.} & \boldsymbol{A}_i \bullet \boldsymbol{X} = b_i, \quad i = 1, \ldots, m, \\ & \mathcal{S}^n \ni \boldsymbol{X} \succeq \boldsymbol{O}, \end{array}\right\} \tag{1}$$

where $\boldsymbol{X}$ is a variable matrix, and $\boldsymbol{A}_i \in \mathcal{S}^n$, $i = 1, \ldots, m$, $\boldsymbol{b} = (b_i) \in \mathbf{R}^m$, and $\boldsymbol{C} \in \mathcal{S}^n$ are constant. The dual of Problem (1) is formulated in variables $\boldsymbol{y} \in \mathbf{R}^m$ as

$$\left.\begin{array}{ll} \max & \boldsymbol{b}^\top \boldsymbol{y}, \\ \text{s.t.} & \boldsymbol{C} - \sum_{i=1}^{m} \boldsymbol{A}_i y_i \succeq \boldsymbol{O}, \end{array}\right\} \tag{2}$$

which is also an SDP problem.

Recently, SDP has received increasing attention for its wide fields of application (Ben-Tal and Nemirovski, 2001; Ohsaki et al., 1999; Wolkowicz et al., 2000). It is well known that *linear program* (LP), *second-order cone program* (SOCP), etc., are included in SDP as the particular cases (Ben-Tal and Nemirovski, 2001). The primal–dual interior-point method, which has been first developed for LP, has been naturally extended to SDP (Kojima et al., 1997; Wolkowicz et al., 2000). It is theoretically guaranteed that the primal–dual interior-point method converges to optimal solutions of the primal–dual pair of SDP Problems (1) and (2) within the number of arithmetic operations bounded by a polynomial of m and n (Ben-Tal and Nemirovski, 2001; Wolkowicz et al., 2000).

2.2. Quasiconvex optimization problem

The α-*sublevel set* of a function $f: \mathbf{R}^n \mapsto \mathbf{R}$ is defined as

$$\mathcal{L}_f(\alpha) = \{\boldsymbol{x} \in \mathbf{R}^n | f(\boldsymbol{x}) \leqslant \alpha\}.$$

A function f is called *quasiconvex* if its domain and all its sublevel sets $\mathcal{L}_f(\alpha)$ for $\alpha \in \mathbf{R}$ are convex.

Let $f_0: \mathbf{R}^n \mapsto \mathbf{R}$ be quasiconvex, and let $f_1, \ldots, f_m: \mathbf{R}^n \mapsto \mathbf{R}$ be convex. The *quasiconvex optimization* problem (Boyd and Vandenberghe, 2004, Section 4.2.5) refers to the optimization problem having the form of

$$\left.\begin{array}{ll} \min & f_0(\boldsymbol{x}), \\ \text{s.t.} & f_i(\boldsymbol{x}) \leqslant 0, \quad i = 1, \ldots, m, \\ & \boldsymbol{A}\boldsymbol{x} = \boldsymbol{b}, \end{array}\right\} \tag{3}$$

where $\boldsymbol{A} \in \mathbf{R}^{m \times n}$ and $\boldsymbol{b} \in \mathbf{R}^m$.

2.3. Technical lemmas

The reminder of this section is devoted to introducing some technical results that will be used in the following sections.

Lemma 2.1 (Homogenization). *Let $\boldsymbol{Q} \in \mathcal{S}^n$, $\boldsymbol{p} \in \mathbf{R}^n$, and $r \in \mathbf{R}$. Then the following two conditions are equivalent*:

(a) $\begin{pmatrix} \boldsymbol{x} \\ 1 \end{pmatrix}^\top \begin{pmatrix} \boldsymbol{Q} & \boldsymbol{p} \\ \boldsymbol{p}^\top & r \end{pmatrix} \begin{pmatrix} \boldsymbol{x} \\ 1 \end{pmatrix} \geqslant 0, \quad \forall \boldsymbol{x} \in \mathbf{R}^n$;

(b) $\begin{pmatrix} \boldsymbol{Q} & \boldsymbol{p} \\ \boldsymbol{p}^\top & r \end{pmatrix} \succeq \boldsymbol{O}$.

Proof. See Lemma A.3 in Calafiore and El Ghaoui (2004). □

Lemma 2.2 ($\mathcal{S}$*-procedure*). *Let $f_0(\boldsymbol{x}), f_1(\boldsymbol{x}), \dots, f_m(\boldsymbol{x})$ be quadratic functions in the variable $\boldsymbol{x} \in \mathbf{R}^n$ defined by*

$$f_i(\boldsymbol{x}) = \boldsymbol{x}^\top \boldsymbol{Q}_i \boldsymbol{x} + 2\boldsymbol{p}_i^\top \boldsymbol{x} + r_i, \quad i = 0, 1, \dots, m,$$

with $\boldsymbol{Q}_i \in \mathcal{S}^n$, $\boldsymbol{p}_i \in \mathbf{R}^n$, and $r_i \in \mathbf{R}$. Then the implication

$$f_1(\boldsymbol{x}) \geqslant 0, \dots, f_m(\boldsymbol{x}) \geqslant 0 \ \Rightarrow \ f_0(\boldsymbol{x}) \geqslant 0 \tag{4}$$

holds if there exist $\tau_1, \dots, \tau_m$ satisfying

$$\tau_1 \geqslant 0, \dots, \tau_m \geqslant 0, \tag{5a}$$

$$f_0(\boldsymbol{x}) - \sum_{i=1}^{m} \tau_i f_i(\boldsymbol{x}) \geqslant 0, \quad \forall \boldsymbol{x} \in \mathbf{R}^n. \tag{5b}$$

Proof. See Boyd et al. (1994, Section 2.6.3) and references therein. □

Lemma 2.2 implies that (5) is a sufficient condition for the implication (4) to be true. Note that there exists a particular case in which (5) is both necessary and sufficient. In Lemma 2.2, suppose $m = 1$ and that there exists an $\boldsymbol{x}'$ satisfying $f_1(\boldsymbol{x}') > 0$. Then (4) holds if and only if there exists a τ_1 satisfying (5). For the proof see Ben-Tal and Nemirovski (2001, Theorem 4.3.3).

3. Separable uncertainties and robustness functions of trusses

Consider a linear elastic truss in three-dimensional space. Small rotations and small strains are assumed. Let $n^{\rm d}$ denote the number of degrees of freedom of displacements; let $\boldsymbol{u} \in \mathbf{R}^{n^{\rm d}}$ and $\boldsymbol{f} \in \mathbf{R}^{n^{\rm d}}$, respectively, denote the vectors of nodal displacements and external forces. The system of equilibrium equations can be written as

$$\boldsymbol{K}\boldsymbol{u} = \boldsymbol{f}, \tag{6}$$

where $\boldsymbol{K} \in \mathcal{S}^{n^{\rm d}}$ denotes the stiffness matrix of the truss.

Let $\boldsymbol{a} = (a_i) \in \mathbf{R}^{n^{\rm m}}$ denote the vector of cross-sectional areas, where $n^{\rm m}$ denotes the number of members. For a truss, it is well known that the stiffness matrix $\boldsymbol{K}$ can be written as

$$\boldsymbol{K}(\boldsymbol{a}) = \sum_{i=1}^{n^{\rm m}} a_i \boldsymbol{K}_i = \sum_{i=1}^{n^{\rm m}} a_i \boldsymbol{b}_i \boldsymbol{b}_i^\top, \tag{7}$$

where $\boldsymbol{K}_i \in \mathcal{S}^{n^{\rm d}}$ and $\boldsymbol{b}_i = (b_{ij}) \in \mathbf{R}^{n^{\rm d}}$, $i = 1, \dots, n^{\rm m}$, are constant matrices and constant vectors.

3.1. Constraints on mechanical performance

Consider mechanical performance of trusses that can be expressed by constraints in terms of displacements. Let $\boldsymbol{Q}_l \in \mathcal{S}^{n^{\mathrm{d}}}$, $\boldsymbol{q}_l \in \mathbf{R}^{n^{\mathrm{d}}}$, and $\gamma_l \in \mathbf{R}$. Suppose that the constraints on mechanical performance can be written in the following quadratic inequalities in terms of $\boldsymbol{u}$:

$$\boldsymbol{u}^{\top}\boldsymbol{Q}_l\boldsymbol{u} + 2\boldsymbol{q}_l^{\top}\boldsymbol{u} + \gamma_l \leqslant 0, \quad l = 1, \dots, n^{\mathrm{c}}, \tag{8}$$

where n^{c} denotes the number of constraints. Let $\boldsymbol{Q}_l$, $\boldsymbol{q}_l$, and γ_l be functions of $\boldsymbol{r}^{\mathrm{c}} \in \mathbf{R}^{n^{\mathrm{r}}}$. Here, $\boldsymbol{r}^{\mathrm{c}}$ is regarded as the vector of parameters representing the levels of performance, and n^{r} denotes the number of these parameters. Define $\boldsymbol{H}_l : \mathbf{R}^{n^{\mathrm{r}}} \mapsto \mathcal{S}^{n^{\mathrm{d}}+1}$ by

$$\boldsymbol{H}_l(\boldsymbol{r}^{\mathrm{c}}) = -\begin{pmatrix} \boldsymbol{Q}_l(\boldsymbol{r}^{\mathrm{c}}) & \boldsymbol{q}_l(\boldsymbol{r}^{\mathrm{c}}) \\ \boldsymbol{q}_l(\boldsymbol{r}^{\mathrm{c}})^{\top} & \gamma_l(\boldsymbol{r}^{\mathrm{c}}) \end{pmatrix}.$$

Letting $\mathcal{P}(\mathbf{R}^{n^{\mathrm{d}}})$ denote the power set of the set $\mathbf{R}^{n^{\mathrm{d}}}$, define a point-to-set mapping $\mathcal{F} : \mathbf{R}^{n^{\mathrm{r}}} \mapsto \mathcal{P}(\mathbf{R}^{n^{\mathrm{d}}})$ by

$$\mathcal{F}(\boldsymbol{r}^{\mathrm{c}}) = \left\{ \boldsymbol{u} \in \mathbf{R}^{n^{\mathrm{d}}} \;\middle|\; \begin{pmatrix} \boldsymbol{u} \\ 1 \end{pmatrix}^{\top} \boldsymbol{H}_l(\boldsymbol{r}^{\mathrm{c}}) \begin{pmatrix} \boldsymbol{u} \\ 1 \end{pmatrix} \geqslant 0, \quad l = 1, \dots, n^{\mathrm{c}} \right\}. \tag{9}$$

Then the constraints (8) are rewritten as

$$\boldsymbol{u} \in \mathcal{F}(\boldsymbol{r}^{\mathrm{c}}). \tag{10}$$

Note that we have restricted ourselves to cases in which the constraints on the truss can be represented by a finite number of quadratic inequalities. However, there exist various constraints that can be described in the form of (9) from a practical point of view, because it is known that any single polynomial inequality can be converted into a system of (a finite number of) quadratic inequalities (see, e.g., Kojima and Tunçel (2000)).

Example 3.1. As an example, we show the explicit reformulation of the stress constraints of trusses into (10). Let E denote the elastic modulus of truss members; let ℓ_i denote the initial unstressed length of the ith member. From (7) it follows that the stress constraints are written as

$$\underline{\sigma}_i^{\mathrm{c}} \leqslant \sqrt{E/\ell_i}\,\boldsymbol{b}_i^{\top}\boldsymbol{u} \leqslant \overline{\sigma}_i^{\mathrm{c}}, \quad i = 1, \dots, n^{\mathrm{m}}, \tag{11}$$

where $\mathbf{R} \ni \underline{\sigma}_i^{\mathrm{c}} < 0$ and $\mathbf{R} \ni \overline{\sigma}_i^{\mathrm{c}} > 0$ denote the lower and upper bounds of stress of the ith member, respectively. Observing that (11) is rewritten as

$$\left| \sqrt{E/\ell_i}\,\boldsymbol{b}_i^{\top}\boldsymbol{u} - \frac{\overline{\sigma}_i^{\mathrm{c}} + \underline{\sigma}_i^{\mathrm{c}}}{2} \right| \leqslant \frac{\overline{\sigma}_i^{\mathrm{c}} - \underline{\sigma}_i^{\mathrm{c}}}{2}, \quad i = 1, \dots, n^{\mathrm{m}},$$

we can embed the stress constraints (11) into the form of (10) with

$$\mathcal{F}(\underline{\boldsymbol{\sigma}}^{\mathrm{c}}, \overline{\boldsymbol{\sigma}}^{\mathrm{c}}) = \left\{ \boldsymbol{u} \in \mathbf{R}^{n^{\mathrm{d}}} \;\middle|\; \begin{pmatrix} \boldsymbol{u} \\ 1 \end{pmatrix}^{\top} \begin{pmatrix} -(E/\ell_i)\boldsymbol{b}_i\boldsymbol{b}_i^{\top} & \dfrac{\sqrt{E/\ell_i}(\overline{\sigma}_i^{\mathrm{c}} + \underline{\sigma}_i^{\mathrm{c}})}{2}\boldsymbol{b}_i \\ \dfrac{\sqrt{E/\ell_i}(\overline{\sigma}_i^{\mathrm{c}} + \underline{\sigma}_i^{\mathrm{c}})}{2}\boldsymbol{b}_i^{\top} & -\overline{\sigma}_i^{\mathrm{c}}\underline{\sigma}_i^{\mathrm{c}} \end{pmatrix} \begin{pmatrix} \boldsymbol{u} \\ 1 \end{pmatrix} \geqslant 0, \quad i = 1, \dots, n^{\mathrm{m}} \right\},$$

where $n^{\mathrm{c}} = n^{\mathrm{m}}$. Note that $(\underline{\boldsymbol{\sigma}}^{\mathrm{c}}, \overline{\boldsymbol{\sigma}}^{\mathrm{c}})$ is regarded as the levels of performance in (11). Hence, we have $\boldsymbol{r}^{\mathrm{c}} = (\underline{\boldsymbol{\sigma}}^{\mathrm{c}}, \overline{\boldsymbol{\sigma}}^{\mathrm{c}})$ with $n^{\mathrm{r}} = 2n^{\mathrm{m}}$. □

3.2. Uncertainty model

Let

$$\boldsymbol{K} = \begin{pmatrix} \boldsymbol{K}_{\rm a} \\ \boldsymbol{K}_{\rm f} \end{pmatrix}, \qquad \boldsymbol{f} = \begin{pmatrix} \boldsymbol{f}_{\rm a} \\ \boldsymbol{f}_{\rm f} \end{pmatrix},$$

with $\boldsymbol{K}_{\rm a} \in \mathbf{R}^{n^{\rm d}_{\rm a} \times n^{\rm d}}$, $\boldsymbol{K}_{\rm f} \in \mathbf{R}^{n^{\rm d}_{\rm f} \times n^{\rm d}}$, $\boldsymbol{f}_{\rm a} \in \mathbf{R}^{n^{\rm d}_{\rm a}}$, and $\boldsymbol{f}_{\rm f} \in \mathbf{R}^{n^{\rm d}_{\rm f}}$, where

$$n^{\rm d}_{\rm a} + n^{\rm d}_{\rm f} = n^{\rm d}.$$

The system (6) of equilibrium equations is rewritten as

$$\boldsymbol{K}_{\rm a}\boldsymbol{u} = \boldsymbol{f}_{\rm a}, \qquad \boldsymbol{K}_{\rm f}\boldsymbol{u} = \boldsymbol{f}_{\rm f}. \tag{12}$$

Similarly, $\boldsymbol{K}_i$ and $\boldsymbol{b}_i$ are decomposed as

$$\boldsymbol{K}_i = \begin{pmatrix} \boldsymbol{K}_{{\rm a}i} \\ \boldsymbol{K}_{{\rm f}i} \end{pmatrix}, \quad \boldsymbol{b}_i = \begin{pmatrix} \boldsymbol{b}_{{\rm a}i} \\ \boldsymbol{b}_{{\rm f}i} \end{pmatrix}, \qquad i = 1, \dots, n^{\rm m}, \tag{13}$$

with $\boldsymbol{K}_{{\rm a}i} \in \mathbf{R}^{n^{\rm d}_{\rm a} \times n^{\rm d}}$, $\boldsymbol{K}_{{\rm f}i} \in \mathbf{R}^{n^{\rm d}_{\rm f} \times n^{\rm d}}$, $\boldsymbol{b}_{{\rm a}i} \in \mathbf{R}^{n^{\rm d}_{\rm a}}$, and $\boldsymbol{b}_{{\rm f}i} \in \mathbf{R}^{n^{\rm d}_{\rm f}}$.

Suppose that $\boldsymbol{f}_{\rm a}$ and $\boldsymbol{K}_{\rm f}$ are the certain vector and matrix, respectively, whereas $\boldsymbol{K}_{\rm a}$ and $\boldsymbol{f}_{\rm f}$ depend on some unknown-but-bounded parameters. We call this uncertainty model of trusses *separable uncertainty*. We further assume that the uncertainty of $\boldsymbol{K}_{\rm a}$ is caused only by the uncertainties of stiffness of $n^{\rm m}_{\rm a}$ members, with the indices $i = 1, \dots, n^{\rm m}_{\rm a}$, where $n^{\rm m}_{\rm a} < n^{\rm m}$. The locations of nodes are assumed to be certain. We describe the uncertainties of member stiffness via the uncertainties of cross-sectional areas of the corresponding $n^{\rm m}_{\rm a}$ members, say, the uncertainties of $a_1, \dots, a_{n^{\rm m}_{\rm a}}$.

Let $\boldsymbol{\zeta}_{\rm a} = (\zeta_{{\rm a}i}) \in \mathbf{R}^{n^{\rm m}_{\rm a}}$ and $\boldsymbol{\zeta}_{\rm f} = (\zeta_{{\rm f}i}) \in \mathbf{R}^{n^{\rm d}_{\rm f}}$ denote the parameter vectors that are considered to be unknown, or, uncertain. We describe the uncertainties of $(a_1, \dots, a_{n^{\rm m}_{\rm a}})$ and $\boldsymbol{f}_{\rm f}$, respectively, by using $\boldsymbol{\zeta}_{\rm a}$ and $\boldsymbol{\zeta}_{\rm f}$.

Example 3.2. Consider a three-bar truss illustrated in Fig. 1. Nodes (a) and (b) are pin-supported. The displacement of node (c) in the direction of the x-axis is constrained, i.e., $n^{\rm d} = 3$. The external forces $f_{\rm a} \in \mathbf{R}$ and $\boldsymbol{f}_{\rm f} \in \mathbf{R}^2$, respectively, are applied at nodes (c) and (d). The cross-sectional areas of members (1), (2), and (3) are denoted by a_1, a_2, and a_3, respectively. Suppose that a_2, a_3, and $f_{\rm a}$ are certain. On the contrary, a_1 and $\boldsymbol{f}_{\rm f}$ are assumed to possess uncertainties in terms of unknown-but-bounded parameters $\zeta_{\rm a1} \in \mathbf{R}$ and $\boldsymbol{\zeta}_{\rm f} \in \mathbf{R}^2$, respectively, i.e.,

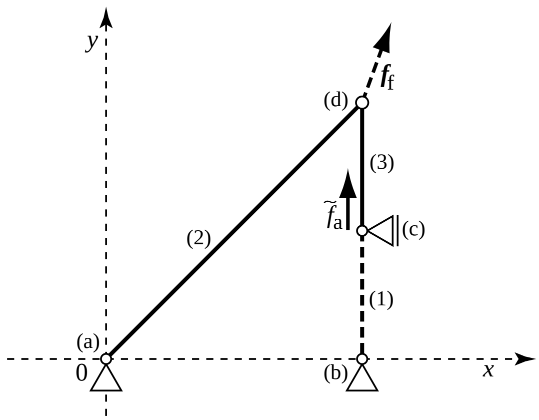

Fig. 1. Three-bar truss.

$$a_1 = \tilde{a}_1 + \delta a_1(\zeta_{a1}), \quad \zeta_{a1} \in \mathscr{Z}_a,$$
$$\boldsymbol{f}_f = \tilde{\boldsymbol{f}}_f + \delta \boldsymbol{f}_f(\boldsymbol{\zeta}_f), \quad \boldsymbol{\zeta}_f \in \mathscr{Z}_f.$$

Here, $\tilde{a}_1 \in \mathbf{R}$ and $\tilde{\boldsymbol{f}}_f \in \mathbf{R}^2$ denote the constant nominal values of a_1 and $\boldsymbol{f}_f$, respectively; $\delta a_1 : \mathbf{R} \mapsto \mathbf{R}$ and $\delta \boldsymbol{f}_f : \mathbf{R}^2 \mapsto \mathbf{R}^2$ denote the perturbation functions of a_1 and $\boldsymbol{f}_f$, respectively; $\mathscr{Z}_a \subset \mathbf{R}$ and $\mathscr{Z}_f \subset \mathbf{R}^2$ denote the given bounded sets. This uncertainty model can be regarded as a separable uncertainty with $n_a^m = 1$, $n_a^d = 1$, and $n_f^d = 2$. Indeed, for this truss, the decomposed equilibrium equations (12) are explicitly written as

$$\left[\frac{E(\tilde{a}_1 + \delta a_1(\zeta_{a1}))}{\ell_1}(1 \quad 0 \quad 0) + \frac{E\tilde{a}_3}{\ell_3}(-1 \quad 0 \quad 0)\right]\boldsymbol{u} = \tilde{f}_a, \tag{14}$$

$$\left[\frac{E\tilde{a}_2}{\ell_2}\begin{pmatrix} 0 & 1/\sqrt{2} & -1/\sqrt{2} \\ 0 & -1/\sqrt{2} & 1/\sqrt{2} \end{pmatrix} + \frac{E\tilde{a}_3}{\ell_3}\begin{pmatrix} 0 & 0 & 0 \\ 0 & 0 & 1 \end{pmatrix}\right]\boldsymbol{u} = \tilde{\boldsymbol{f}}_f + \delta \boldsymbol{f}_f(\boldsymbol{\zeta}_f), \tag{15}$$

where ζ_{a1} and $\boldsymbol{\zeta}_f$ are the uncertain parameters, and $\boldsymbol{u}$ is the variable vector. Thus, we can see that (14) and (15) include, respectively, the uncertain parameters only on the left-hand side matrix and right-hand side vector, which validates that the truss obeys the separable uncertainty model. □

Let $\tilde{\boldsymbol{a}} = (\tilde{a}_i)$, $\tilde{\boldsymbol{f}}_f$, and $\tilde{\boldsymbol{f}}_a$ denote the nominal values of $\boldsymbol{a}$, $\boldsymbol{f}_f$, and $\boldsymbol{f}_a$, respectively. Consider the following uncertainty model:

$$a_i = \tilde{a}_i + a_i^0 \zeta_{ai}, \quad i = 1, \ldots, n_a^m,$$
$$\boldsymbol{f}_f = \tilde{\boldsymbol{f}}_f + f^0 \boldsymbol{\zeta}_f,$$

where $a_1^0, \ldots, a_{n_a^m}^0 \geqslant 0$ and $f^0 \geqslant 0$ are constant coefficients representing the relative magnitudes of uncertainties of $a_1, \ldots, a_{n_a^m}$ and $\boldsymbol{f}_f$, respectively. We further assume that $a_{n_a^m+1}, \ldots, a_{n^m}$ and $\boldsymbol{f}_a$ are certain. For simplicity, we write

$$\widetilde{\boldsymbol{K}}_a := \boldsymbol{K}_a(\tilde{\boldsymbol{a}}), \qquad \widetilde{\boldsymbol{K}}_f := \boldsymbol{K}_f(\tilde{\boldsymbol{a}}).$$

Then we achieve the following separable uncertainty model of $\boldsymbol{K}$ and $\boldsymbol{f}$:

$$\boldsymbol{K}_a = \widetilde{\boldsymbol{K}}_a + \sum_{i=1}^{n_a^m} a_i^0 \zeta_{ai} \boldsymbol{K}_{ai}, \quad \boldsymbol{f}_a = \tilde{\boldsymbol{f}}_a, \tag{16}$$

$$\boldsymbol{K}_f = \widetilde{\boldsymbol{K}}_f, \quad \boldsymbol{f}_f = \tilde{\boldsymbol{f}}_f + f^0 \boldsymbol{\zeta}_f, \tag{17}$$

where $\boldsymbol{\zeta}_a \in \mathbf{R}^{n_a^m}$ and $\boldsymbol{\zeta}_f \in \mathbf{R}^{n_f^d}$ are the uncertainty parameters. Define two point-to-set mappings $\mathscr{Z}_a$: $\mathbf{R}_+ \mapsto \mathscr{P}(\mathbf{R}^{n_a^m})$ and $\mathscr{Z}_f : \mathbf{R}_+ \mapsto \mathscr{P}(\mathbf{R}^{n_f^d})$ by

$$\mathscr{Z}_a(\alpha) = \{\boldsymbol{\zeta} \in \mathbf{R}^{n_a^m} | \alpha \geqslant \|\boldsymbol{\zeta}\|_\infty\}, \tag{18}$$

$$\mathscr{Z}_f(\alpha) = \{\boldsymbol{\zeta} \in \mathbf{R}^{n_f^d} | \alpha \geqslant \|\boldsymbol{\zeta}\|_2\}. \tag{19}$$

For a given $\alpha \geqslant 0$, the uncertain parameters $\boldsymbol{\zeta}_a$ and $\boldsymbol{\zeta}_f$ in (16) and (17), respectively, are assumed to be running through *uncertain sets* $\mathscr{Z}_a(\alpha)$ and $\mathscr{Z}_f(\alpha)$ defined by (18) and (19). Roughly speaking, $\boldsymbol{\zeta}_a \in \mathscr{Z}_a(\alpha)$ and $\boldsymbol{\zeta}_f \in \mathscr{Z}_f(\alpha)$ perturb around the origin with the 'width' of α.

Remark 3.3. Note that we have used the l_∞- and l_2-norms, respectively, in order to define $\mathscr{Z}_a$ and $\mathscr{Z}_f$ in (18) and (19). There exist several reasons why we choose these norms. Recall that ζ_{ai} describes the uncertainty of stiffness of the ith member. Since a truss is an assemblage of nodes connected by some independent members, the perturbation of stiffness of a member from its nominal value does not affect those of the other members. Hence, we choose the l_∞-norm which represents the independent uncertainties of scalars $\zeta_{a1}, \ldots, \zeta_{an_a^m}$. Moreover, the assumption (18) is necessary for our approach. Precisely, we shall use a specific characteristic of the l_∞-norm in the proof of Proposition 4.2. On the contrary, it is not easy to justify what kind of uncertainty set should be used for $\boldsymbol{\zeta}_f$ from the mechanical point of view. This is because there exist various phenomena that may possibly cause the uncertainty of external forces. We have used the l_2-norm in (19) as one of adequate choices. In addition, using the l_2-norm makes the presentation in Section 4 simple. The l_∞-norm can be an alternative choice that also seems to be adequate, i.e., letting

$$\mathscr{Z}_f^{\rm int}(\alpha) = \left\{ \boldsymbol{\zeta} \in \mathbf{R}^{n_f^d} | \alpha \geqslant \|\boldsymbol{\zeta}\|_\infty \right\}, \tag{20}$$

we may assume $\boldsymbol{\zeta}_f \in \mathscr{Z}_f^{\rm int}(\alpha)$. The uncertainty set $\mathscr{Z}_f^{\rm int}$ is conventionally used in interval analyses of structures (see, e.g., Muhanna and Mullen, 2001). We shall show in Remark 4.5 that $\mathscr{Z}_f^{\rm int}$ can be dealt with by our approach developed in Section 4. However, we use $\mathscr{Z}_f$ for presenting our main result in Section 4 for simplicity. From the point of view of numerical computation, using $\mathscr{Z}_f$ has an advantage that the optimization problems solved in our algorithm have less numerical complexity compared with the case where we use $\mathscr{Z}_f^{\rm int}$. Indeed, $\mathscr{Z}_f^{\rm int}$ requires more variables in our formulation, which is discussed in Remark 4.7. □

Consequently, the system (6) of equilibrium equations is reduced to

$$\widetilde{\boldsymbol{K}}_a \boldsymbol{u} - \tilde{\boldsymbol{f}}_a = -\sum_{i=1}^{n_a^m} a_i^0 \zeta_{ai} \boldsymbol{K}_{ai} \boldsymbol{u}, \quad \boldsymbol{\zeta}_a \in \mathscr{Z}_a(\alpha), \tag{21}$$

$$\widetilde{\boldsymbol{K}}_f \boldsymbol{u} - \tilde{\boldsymbol{f}}_f = f^0 \boldsymbol{\zeta}_f, \quad \boldsymbol{\zeta}_f \in \mathscr{Z}_f(\alpha). \tag{22}$$

Let $\mathscr{U}(\alpha, \tilde{\boldsymbol{a}}) \subset \mathbf{R}^{n^d}$ denote the set of all the possible solutions to (21) and (22), i.e., $\mathscr{U}$ is the point-to-set mapping $\mathscr{U} : \mathbf{R}_+ \times \mathbf{R}^{n^m} \mapsto \mathscr{P}(\mathbf{R}^{n^d})$ defined by

$$\mathscr{U}(\alpha, \tilde{\boldsymbol{a}}) = \{ \boldsymbol{u} \in \mathbf{R}^{n^d} \mid (21), (22) \}. \tag{23}$$

3.3. Robustness function

In this section, we show that the robustness function (Ben-Haim, 2001) of trusses is obtained as the optimal objective value of a mathematical programming problem with infinitely many constraint conditions. For calculating the robustness function of a simple illustrative truss, see Kanno and Takewaki (2004a, Section 3).

It is easy to see that the uncertainty sets $\mathscr{Z}_a$ and $\mathscr{Z}_f$ defined by (18) and (19) obey so-called *info-gap models* (Ben-Haim, 2001). Especially, they satisfy the axioms of nesting and contraction (Ben-Haim, 2001, Section 2.5), i.e., we see (i) $\mathscr{Z}_a(\alpha_1) \subset \mathscr{Z}_a(\alpha_2)$ and $\mathscr{Z}_f(\alpha_1) \subset \mathscr{Z}_f(\alpha_2)$ if $0 \leqslant \alpha_1 < \alpha_2$; (ii) $\mathscr{Z}_a(0) = \{\boldsymbol{\zeta}_a \mid \boldsymbol{\zeta}_a = \mathbf{0}\}$ and $\mathscr{Z}_f(0) = \{\boldsymbol{\zeta}_f \mid \boldsymbol{\zeta}_f = \mathbf{0}\}$.

Consider the following *semi-infinite programming* problem:

$$\alpha^* = \max \{ \alpha : \boldsymbol{u} \in \mathscr{F}(\boldsymbol{r}^c), \ \forall \boldsymbol{u} \in \mathscr{U}(\alpha, \tilde{\boldsymbol{a}}) \}, \tag{24}$$

where $\mathscr{F}$ and $\mathscr{U}$ have been defined in (9) and (23), respectively. Here, by *semi-infinite* we mean optimization problems having a finite number of scalar variables and possibly an infinite number of inequality constraints. Note that α^* defined by (24) depends on the level $\boldsymbol{r}^c$ of constraints on mechanical performance as well as the nominal cross-sectional areas $\tilde{\boldsymbol{a}}$.

The robustness function $\hat{\alpha} : \mathbf{R}^{n^m} \times \mathbf{R}^{n^r} \mapsto (-\infty, +\infty]$ associated with the constraints (8) is defined by (Ben-Haim, 2001, Chapter 3)

$$\hat{\alpha}(\tilde{\boldsymbol{a}}, \boldsymbol{r}^c) = \begin{cases} \alpha^* & \text{if Problem (24) is feasible}, \\ 0 & \text{if Problem (24) is infeasible}. \end{cases} \tag{25}$$

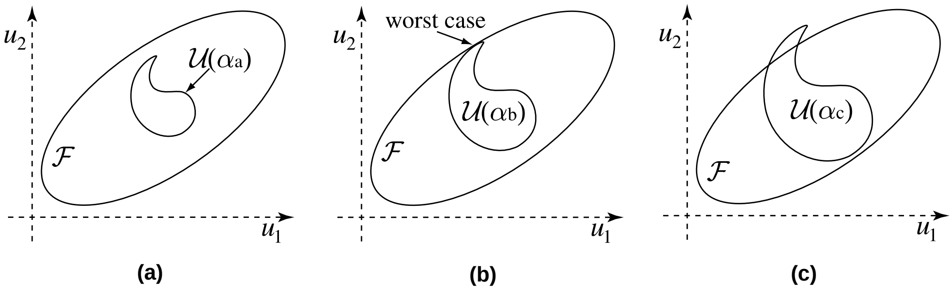

Fig. 2. Relation among $\mathscr{F}(\boldsymbol{r}^c)$, $\mathscr{U}(\alpha, \tilde{\boldsymbol{a}})$, and $\hat{\alpha}$ with various α: (a) $\alpha_a < \hat{\alpha}$, (b) $\alpha_b = \hat{\alpha}$, and (c) $\alpha_c > \hat{\alpha}$.

Throughout the paper, we assume $\mathscr{U}(0, \tilde{\boldsymbol{a}}) \subseteq \mathscr{F}(\boldsymbol{r}^c)$ for simplicity, and hence Problem (24) is feasible. In what follows, $\hat{\alpha}(\tilde{\boldsymbol{a}}, \boldsymbol{r}^c)$ is often abbreviated by $\hat{\alpha}$ or $\hat{\alpha}(\tilde{\boldsymbol{a}})$.

The concept of *robust feasibility* has been used in the literature of robust optimization (see, e.g., Ben-Tal and Nemirovski, 2002). Note that $\alpha = 0$ implies that $\boldsymbol{K}$ and $\boldsymbol{f}$ have no uncertainties. For the fixed $\tilde{\boldsymbol{a}} \in \mathbf{R}^{n^m}$, $\mathscr{U}(0, \tilde{\boldsymbol{a}})$ is a single point corresponding to the displacements vector, if $\widetilde{\boldsymbol{K}}$ has a full row rank. Hence, $\tilde{\boldsymbol{a}}$ is a feasible solution in the usual sense if $\boldsymbol{u} \in \mathscr{U}(0, \tilde{\boldsymbol{a}})$ satisfies $\boldsymbol{u} \in \mathscr{F}(\boldsymbol{r}^c)$. For the fixed $\alpha' > 0$, $\tilde{\boldsymbol{a}}$ is regarded as a robust feasible solution if $\boldsymbol{u} \in \mathscr{F}(\tilde{\boldsymbol{a}}, \boldsymbol{r}^c)$ satisfies $\boldsymbol{u} \in \mathscr{F}(\boldsymbol{r}^c)$ for all possible realizations $\boldsymbol{\zeta}_a \in \mathscr{Z}_a(\alpha')$ and $\boldsymbol{\zeta}_f \in \mathscr{Z}_f(\alpha')$. What we are seeking for in (24) is the maximum value of α such that $\tilde{\boldsymbol{a}}$ remains to be a robust feasible solution.

For the two different vectors of design variables $\tilde{\boldsymbol{a}}^1 \in \mathbf{R}^{n^m}$ and $\tilde{\boldsymbol{a}}^2 \in \mathbf{R}^{n^m}$, we say that $\tilde{\boldsymbol{a}}^1$ is *more robust* than $\tilde{\boldsymbol{a}}^2$ if $\hat{\alpha}(\tilde{\boldsymbol{a}}^1, \boldsymbol{r}^c) > \hat{\alpha}(\tilde{\boldsymbol{a}}^2, \boldsymbol{r}^c)$. Let $\boldsymbol{u}^1 \in \mathscr{U}(\hat{\alpha}, \tilde{\boldsymbol{a}}^1)$ at $\boldsymbol{\zeta}_a^1 \in \mathscr{Z}_a(\hat{\alpha})$ and $\boldsymbol{\zeta}_f^1 \in \mathscr{Z}_f(\hat{\alpha})$. If there exists an $l \in \{1, \ldots, n^c\}$ satisfying

$$(\boldsymbol{u}^1)^\top \boldsymbol{Q}_l(\boldsymbol{r}^c)\boldsymbol{u}^1 + 2\boldsymbol{q}_l(\boldsymbol{r}^c)^\top \boldsymbol{u}^1 + \gamma_l(\boldsymbol{r}^c) = 0,$$

then we say that $(\boldsymbol{\zeta}_a^1, \boldsymbol{\zeta}_f^1)$ is the *worst case*. Note that there exists typically more than a single worst case. Especially, optimum truss designs maximizing the robustness function or for specified robustness function often have many worst cases (Kanno and Takewaki, 2004b).

Fig. 2 illustrates the relation among $\mathscr{F}(\boldsymbol{r}^c)$, $\mathscr{U}(\alpha, \tilde{\boldsymbol{a}})$, and $\hat{\alpha}$ with various values of α. Here, Fig. 2(a) and (b), respectively, correspond to $\alpha_a < \hat{\alpha}$ and $\alpha_b = \hat{\alpha}$, where we see that the constraint $\boldsymbol{u} \in \mathscr{F}(\boldsymbol{u}^c)$ is satisfied for all possible $\boldsymbol{u} \in \mathscr{U}(\alpha, \tilde{\boldsymbol{a}})$. The worst case corresponds to the point $\boldsymbol{u} \in \mathscr{U}(\hat{\alpha}, \tilde{\boldsymbol{a}})$ on the boundary of $\mathscr{F}(\boldsymbol{r}^c)$ in Fig. 2(b). It is observed in Fig. 2(c) that some solutions $\boldsymbol{u} \in \mathscr{U}(\alpha_c, \tilde{\boldsymbol{a}})$ to the equilibrium equations violate the constraint $\boldsymbol{u} \in \mathscr{F}(\boldsymbol{r}^c)$, which implies $\alpha_c > \hat{\alpha}$.

Consequently, the robustness function $\hat{\alpha}$ can be obtained by solving the optimization problem (24). However, it should be emphasized that Problem (24) is numerically intractable, because it has infinitely many constraints. This motivates us to develop an approximation algorithm for solving Problem (24), which provides a lower bound of the robustness function.

4. Lower bounds of robustness functions

In this section, we propose an approximation algorithm for Problem (24), which provides a lower bound on the robustness function $\hat{\alpha}(\tilde{\boldsymbol{a}}, \boldsymbol{r}^c)$. Note that finding a lower bound on the robustness function is more significant than finding an upper bound, since a lower bound is regarded as a conservative estimation of the robustness function, i.e., as a level of uncertainty at which the constraints of mechanical performance are guaranteed not to be violated.

We start with embedding (22) into a quadratic inequality.

Proposition 4.1. *The condition (22) is equivalent to*

$$\begin{pmatrix} \boldsymbol{u} \\ 1 \end{pmatrix}^{\top} \begin{pmatrix} -\widetilde{\boldsymbol{K}}_{\rm f}^{\top}\widetilde{\boldsymbol{K}}_{\rm f} & \widetilde{\boldsymbol{K}}_{\rm f}^{\top}\tilde{\boldsymbol{f}}_{\rm f} \\ \tilde{\boldsymbol{f}}_{\rm f}^{\top}\widetilde{\boldsymbol{K}}_{\rm f} & (f^0\alpha)^2 - \tilde{\boldsymbol{f}}_{\rm f}^{\top}\tilde{\boldsymbol{f}}_{\rm f} \end{pmatrix} \begin{pmatrix} \boldsymbol{u} \\ 1 \end{pmatrix} \geqslant 0. \tag{26}$$

Proof. From the definition (19) of $\mathscr{Z}_{\rm f}(\alpha)$, it is easy to see that (22) is equivalent to

$$(\widetilde{\boldsymbol{K}}_{\rm f}\boldsymbol{u} - \tilde{\boldsymbol{f}}_{\rm f})^{\top}(\widetilde{\boldsymbol{K}}_{\rm f}\boldsymbol{u} - \tilde{\boldsymbol{f}}_{\rm f}) \leqslant (f^0\alpha)^2,$$

which can be rewritten as (26). □

We next embed (21) into a quadratic inequality. Define the matrix $\boldsymbol{\Psi} \in \mathbf{R}^{n_{\rm a}^{\rm d} \times n_{\rm a}^{\rm m}}$ by

$$\boldsymbol{\Psi} = (\boldsymbol{b}_{{\rm a}1}, \ldots, \boldsymbol{b}_{{\rm a}n_{\rm a}^{\rm m}}),$$

where $\boldsymbol{b}_{{\rm a}i}$ is defined in (13). In what follows, we assume

$$n_{\rm a}^{\rm d} \leqslant n_{\rm a}^{\rm m},$$

which is usually satisfied for trusses. Let

$$n^{\rm n} = n_{\rm a}^{\rm m} - {\rm rank}\,\boldsymbol{\Psi}, \tag{27}$$

where ${\rm rank}\,\boldsymbol{\Psi}$ denotes the row rank of $\boldsymbol{\Psi}$. Then we see $n^{\rm n} \geqslant 0$.

Let $\boldsymbol{\Psi}^{\dagger} \in \mathbf{R}^{n_{\rm a}^{\rm m} \times n_{\rm a}^{\rm d}}$ denote the pseudo-inverse of $\boldsymbol{\Psi}$. $\boldsymbol{\Psi}^{\perp} \in \mathbf{R}^{n_{\rm a}^{\rm m} \times n^{\rm n}}$ denotes a basis for the nullspace of $\boldsymbol{\Psi}$, where the nullspace of $\boldsymbol{\Psi}$ is the set of all vectors $\boldsymbol{\eta} \in \mathbf{R}^{n_{\rm a}^{\rm m}}$ satisfying $\boldsymbol{\Psi}\boldsymbol{\eta} = \mathbf{0}$. For $n^{\rm n} \geqslant 1$, letting $\boldsymbol{v} \in \mathbf{R}^{n^{\rm n}}$, define $\boldsymbol{\xi} \in \mathbf{R}^{n^{\rm n}+n^{\rm d}+1}$ and $\boldsymbol{\Omega}_{{\rm a}i}(\alpha^2) \in \mathscr{S}^{n^{\rm n}+n^{\rm d}+1}$, $i = 1, \ldots, n_{\rm a}^{\rm m}$, by

$$\boldsymbol{\xi} = (\boldsymbol{v}, \boldsymbol{u}, 1),$$

$$\boldsymbol{\Omega}_{{\rm a}i}(\alpha^2) = \alpha^2 \begin{pmatrix} \boldsymbol{O} & \boldsymbol{O} & \mathbf{0} \\ \boldsymbol{O} & (a_i^0)^2\boldsymbol{b}_i\boldsymbol{b}_i^{\top} & \mathbf{0} \\ \mathbf{0}^{\top} & \mathbf{0}^{\top} & 0 \end{pmatrix} + \begin{pmatrix} -(\boldsymbol{\Psi}_{i,\cdot}^{\perp})^{\top}\boldsymbol{\Psi}_{i,\cdot}^{\perp} & -(\boldsymbol{\Psi}_{i,\cdot}^{\perp})^{\top}\boldsymbol{\Psi}_{i,\cdot}^{\dagger}\widetilde{\boldsymbol{K}}_{\rm a} & (\boldsymbol{\Psi}_{i,\cdot}^{\dagger}\tilde{\boldsymbol{f}}_{\rm a})(\boldsymbol{\Psi}_{i,\cdot}^{\perp})^{\top} \\ -(\boldsymbol{\Psi}_{i,\cdot}^{\dagger}\widetilde{\boldsymbol{K}}_{\rm a})^{\top}\boldsymbol{\Psi}_{i,\cdot}^{\perp} & -(\boldsymbol{\Psi}_{i,\cdot}^{\dagger}\widetilde{\boldsymbol{K}}_{\rm a})^{\top}(\boldsymbol{\Psi}_{i,\cdot}^{\dagger}\widetilde{\boldsymbol{K}}_{\rm a}) & (\boldsymbol{\Psi}_{i,\cdot}^{\dagger}\tilde{\boldsymbol{f}}_{\rm a})(\boldsymbol{\Psi}_{i,\cdot}^{\dagger}\widetilde{\boldsymbol{K}}_{\rm a})^{\top} \\ (\boldsymbol{\Psi}_{i,\cdot}^{\dagger}\tilde{\boldsymbol{f}}_{\rm a})\boldsymbol{\Psi}_{i,\cdot}^{\perp} & (\boldsymbol{\Psi}_{i,\cdot}^{\dagger}\tilde{\boldsymbol{f}}_{\rm a})\boldsymbol{\Psi}_{i,\cdot}^{\dagger}\widetilde{\boldsymbol{K}}_{\rm a} & -(\boldsymbol{\Psi}_{i,\cdot}^{\dagger}\tilde{\boldsymbol{f}}_{\rm a})^2 \end{pmatrix},$$

where $\boldsymbol{\Psi}_{i,\cdot}^{\dagger}$ and $\boldsymbol{\Psi}_{i,\cdot}^{\perp}$ denote the ith row vectors of $\boldsymbol{\Psi}^{\dagger}$ and $\boldsymbol{\Psi}^{\perp}$, respectively. Alternatively, for $n^{\rm n} = 0$, define $\boldsymbol{\xi}$ and $\boldsymbol{\Omega}_{{\rm a}i}$ as

$$\boldsymbol{\xi} = (\boldsymbol{u}, 1),$$

$$\boldsymbol{\Omega}_{{\rm a}i}(\alpha^2) = \alpha^2 \begin{pmatrix} (a_i^0)^2\boldsymbol{b}_i\boldsymbol{b}_i^{\top} & \mathbf{0} \\ \mathbf{0}^{\top} & 0 \end{pmatrix} + \begin{pmatrix} -(\boldsymbol{\Psi}_{i,\cdot}^{\dagger}\widetilde{\boldsymbol{K}}_{\rm a})^{\top}(\boldsymbol{\Psi}_{i,\cdot}^{\dagger}\widetilde{\boldsymbol{K}}_{\rm a}) & (\boldsymbol{\Psi}_{i,\cdot}^{\dagger}\tilde{\boldsymbol{f}}_{\rm a})(\boldsymbol{\Psi}_{i,\cdot}^{\dagger}\widetilde{\boldsymbol{K}}_{\rm a})^{\top} \\ (\boldsymbol{\Psi}_{i,\cdot}^{\dagger}\tilde{\boldsymbol{f}}_{\rm a})\boldsymbol{\Psi}_{i,\cdot}^{\dagger}\widetilde{\boldsymbol{K}}_{\rm a} & -(\boldsymbol{\Psi}_{i,\cdot}^{\dagger}\tilde{\boldsymbol{f}}_{\rm a})^2 \end{pmatrix}.$$

The following proposition shows the reduction of (21) into a quadratic inequality:

Proposition 4.2. *The condition (21) is equivalent to*

$$\boldsymbol{\xi}^{\top}\boldsymbol{\Omega}_{{\rm a}i}(\alpha^2)\boldsymbol{\xi} \geqslant 0, \quad i = 1, \ldots, n_{\rm a}^{\rm m}. \tag{28}$$

Proof. From (7) and (13), $\boldsymbol{K}_{{\rm a}i}$ is rewritten as $\boldsymbol{K}_{{\rm a}i} = \boldsymbol{b}_{{\rm a}i}\boldsymbol{b}_i^{\top}$. Hence, we see

$$\sum_{i=1}^{n_{\rm a}^{\rm m}} a_i^0\zeta_{{\rm a}i}\boldsymbol{K}_{{\rm a}i}\boldsymbol{u} = \sum_{i=1}^{n_{\rm a}^{\rm m}} a_i^0\zeta_{{\rm a}i}\boldsymbol{b}_{{\rm a}i}\boldsymbol{b}_i^{\top}\boldsymbol{u} = (\boldsymbol{b}_{{\rm a}1}, \ldots, \boldsymbol{b}_{{\rm a}n_{\rm a}^{\rm m}})\,{\rm diag}(a_i^0\zeta_{{\rm a}i}) \begin{pmatrix} \boldsymbol{b}_1^{\top}\boldsymbol{u} \\ \cdots \\ \boldsymbol{b}_{n_{\rm a}^{\rm m}}^{\top}\boldsymbol{u} \end{pmatrix}. \tag{29}$$

By using (29), the equality in (21) is reduced to

$$\widetilde{\boldsymbol{K}}_{\mathrm{a}}\boldsymbol{u} - \tilde{\boldsymbol{f}}_{\mathrm{a}} = -\boldsymbol{\Psi}\,\mathrm{diag}(a_i^0\zeta_{\mathrm{a}i})\begin{pmatrix} \boldsymbol{b}_1^\top \boldsymbol{u} \\ \cdots \\ \boldsymbol{b}_{n_{\mathrm{a}}^{\mathrm{m}}}^\top \boldsymbol{u} \end{pmatrix},$$

from which it follows that the uncertain system (21) is equivalent to

$$\boldsymbol{\Psi}\boldsymbol{w} = \widetilde{\boldsymbol{K}}_{\mathrm{a}}\boldsymbol{u} - \tilde{\boldsymbol{f}}_{\mathrm{a}}, \tag{30}$$

$$w_i = \zeta_{\mathrm{a}i}(-a_i^0\boldsymbol{b}_i^\top\boldsymbol{u}), \quad \alpha \geqslant |\zeta_{\mathrm{a}i}|, \ \ i = 1, \ldots, n_{\mathrm{a}}^{\mathrm{m}}. \tag{31}$$

Here, $\boldsymbol{w} = (w_i) \in \mathbf{R}^{n^{\mathrm{m}}}$ is an auxiliary variable vector. Observe that, for $p \in \mathbf{R}$ and $q \in \mathbf{R}$, the implication

$$p = \zeta_{\mathrm{a}i}q, \quad \alpha \geqslant |\zeta_{\mathrm{a}i}| \iff p^2 \leqslant \alpha^2 q^2$$

holds, from which it follows that (31) is equivalent to

$$w_i^2 \leqslant (a_i^0\alpha)^2(\boldsymbol{b}_i^\top\boldsymbol{u})^2, \quad i = 1, \ldots, n_{\mathrm{a}}^{\mathrm{m}}. \tag{32}$$

Moreover, we see that any solution to (30) can be written as

$$\boldsymbol{w} = \boldsymbol{\Psi}^\dagger(\widetilde{\boldsymbol{K}}_{\mathrm{a}}\boldsymbol{u} - \tilde{\boldsymbol{f}}_{\mathrm{a}}) + \boldsymbol{\Psi}^\perp\boldsymbol{v} \tag{33}$$

with $\boldsymbol{v} \in \mathbf{R}^{n^{\mathrm{n}}}$. Consequently, by using (32) and (33), we see that (30) and (31) are equivalent to

$$(a_i^0\alpha)^2(\boldsymbol{b}_i^\top\boldsymbol{u})^2 - [\boldsymbol{\Psi}_{i,\cdot}^\dagger(\widetilde{\boldsymbol{K}}_{\mathrm{a}}\boldsymbol{u} - \tilde{\boldsymbol{f}}_{\mathrm{a}}) + \boldsymbol{\Psi}_{i,\cdot}^\perp\boldsymbol{v}]^2 \geqslant 0, \quad i = 1, \ldots, n_{\mathrm{a}}^{\mathrm{m}},$$

which can be rewritten as (28). □

For $\alpha \in \mathbf{R}_+$ and $\boldsymbol{r}^{\mathrm{c}} \in \mathbf{R}^{n^{\mathrm{r}}}$, define $\boldsymbol{\Omega}_{\mathrm{f}}(\alpha^2) \in \mathscr{S}^{n^{\mathrm{n}}+n^{\mathrm{d}}+1}$ and $\boldsymbol{H}_l'(\boldsymbol{r}^{\mathrm{c}}) \in \mathscr{S}^{n^{\mathrm{n}}+n^{\mathrm{d}}+1}$, $l = 1, \ldots, n^{\mathrm{c}}$, by

$$\boldsymbol{\Omega}_{\mathrm{f}}(\alpha^2) = \begin{pmatrix} \boldsymbol{O} & \boldsymbol{O} & \boldsymbol{0} \\ \boldsymbol{O} & -\widetilde{\boldsymbol{K}}_{\mathrm{f}}^\top\widetilde{\boldsymbol{K}}_{\mathrm{f}} & \widetilde{\boldsymbol{K}}_{\mathrm{f}}^\top\tilde{\boldsymbol{f}}_{\mathrm{f}} \\ \boldsymbol{0}^\top & \tilde{\boldsymbol{f}}_{\mathrm{f}}^\top\widetilde{\boldsymbol{K}}_{\mathrm{f}} & (f^0)^2\alpha^2 - \tilde{\boldsymbol{f}}_{\mathrm{f}}^\top\tilde{\boldsymbol{f}}_{\mathrm{f}} \end{pmatrix},$$

$$\boldsymbol{H}_l'(\boldsymbol{r}^{\mathrm{c}}) = \begin{pmatrix} \boldsymbol{O} & \boldsymbol{O} \\ \boldsymbol{O} & \boldsymbol{H}_l \end{pmatrix}, \quad l = 1, \ldots, n^{\mathrm{c}},$$

so that we obtain

$$(26) \iff \boldsymbol{\xi}^\top\boldsymbol{\Omega}_{\mathrm{f}}(\alpha^2)\boldsymbol{\xi} \geqslant 0,$$

$$(8) \iff \boldsymbol{\xi}^\top\boldsymbol{H}_l'(\boldsymbol{r}^{\mathrm{c}})\boldsymbol{\xi} \geqslant 0, \quad l = 1, \ldots, n^{\mathrm{c}}.$$

The following proposition, which plays a key role in constructing a relaxation of Problem (24), shows a relaxation of infinitely many constraints by using a finite number of constraints:

Proposition 4.3. *The implication*

$$\boldsymbol{u} \in \mathscr{U}(\alpha, \tilde{\boldsymbol{a}}) \ \Rightarrow \ \boldsymbol{u} \in \mathscr{F}(\boldsymbol{r}^{\mathrm{c}}) \tag{34}$$

holds if there exist ρ_l *and* $(\tau_{1l}, \ldots, \tau_{n_{\mathrm{a}}^{\mathrm{m}}l})$, $l = 1, \ldots, n^{c}$, *satisfying*

$$\boldsymbol{H}_l'(\boldsymbol{r}^{\mathrm{c}}) - \rho_l\boldsymbol{\Omega}_{\mathrm{f}}(\alpha^2) - \sum_{i=1}^{n_{\mathrm{a}}^{\mathrm{m}}}\tau_{il}\boldsymbol{\Omega}_{\mathrm{a}i}(\alpha^2) \succeq \boldsymbol{O}, \quad l = 1, \ldots, n^{\mathrm{c}}, \tag{35}$$

$$\rho_l \geqslant 0, \quad \tau_{1l}, \ldots, \tau_{n_{\mathrm{a}}^{\mathrm{m}}l} \geqslant 0, \quad l = 1, \ldots, n^{\mathrm{c}}. \tag{36}$$

Proof. From Propositions 4.1 and 4.2 it follows that the system of (21) and (22) is equivalent to

$$\boldsymbol{\xi}^{\top}\boldsymbol{\Omega}_{\mathrm{f}}\boldsymbol{\xi} \geqslant 0, \qquad \boldsymbol{\xi}^{\top}\boldsymbol{\Omega}_{\mathrm{a}i}\boldsymbol{\xi} \geqslant 0, \quad i = 1, \ldots, n_{\mathrm{a}}^{\mathrm{m}}.$$

Observe that the constraints (8) are reduced to

$$\boldsymbol{\xi}^{\top}\boldsymbol{H}_l'\boldsymbol{\xi} \geqslant 0, \quad l = 1, \ldots, n^{\mathrm{c}}.$$

Consequently, the implication (34) holds if and only if the implication

$$\boldsymbol{\xi}^{\top}\boldsymbol{\Omega}_{\mathrm{f}}\boldsymbol{\xi} \geqslant 0, \quad \boldsymbol{\xi}^{\top}\boldsymbol{\Omega}_{\mathrm{a}i}\boldsymbol{\xi} \geqslant 0, \; i = 1, \ldots, n_{\mathrm{a}}^{\mathrm{m}} \;\; \Rightarrow \;\; \boldsymbol{\xi}^{\top}\boldsymbol{H}_l'\boldsymbol{\xi} \geqslant 0 \tag{37}$$

holds for each $l = 1, \ldots, n^{\mathrm{c}}$. The assertion of this proposition is obtained by applying Lemmas 2.1 and Lemma 2.2 to (37). □

Fig. 3 illustrates the relation among the three propositions presented in this section. By using Propositions 4.1, 4.2, 4.3, we have shown that the set of constraints (35) and (36) is a sufficient condition for the infinitely many constraints of Problem (24) to be satisfied. Based on this sufficient condition, we next construct lower bounds of Problem (24).

Lemma 4.4. *Consider the following problem in variables* $(t, \boldsymbol{\rho}, \boldsymbol{\tau}) \in \mathbf{R} \times \mathbf{R}^{n^{\mathrm{c}}} \times \mathbf{R}^{n_{\mathrm{a}}^{\mathrm{m}} n^{\mathrm{c}}}$ *with* $\boldsymbol{\rho} = (\rho_1, \ldots, \rho_{n^{\mathrm{c}}})$ *and* $\boldsymbol{\tau} = (\tau_{11}, \ldots, \tau_{n_{\mathrm{a}}^{\mathrm{m}}1}, \ldots, \tau_{1n^{\mathrm{c}}}, \ldots, \tau_{n_{\mathrm{a}}^{\mathrm{m}}n^{\mathrm{c}}})$:

$$t^* := \max\left\{ t : \boldsymbol{H}_l' - \rho_l \boldsymbol{\Omega}_{\mathrm{f}}(t) - \sum_{i=1}^{n_{\mathrm{a}}^{\mathrm{m}}} \tau_{il} \boldsymbol{\Omega}_{\mathrm{a}i}(t) \succeq \boldsymbol{O}, \;\; \rho_l \geqslant 0, \; \tau_{1l}, \ldots, \tau_{n_{\mathrm{a}}^{\mathrm{m}}l} \geqslant 0, \;\; l = 1, \ldots, n^{\mathrm{c}} \right\}. \tag{38}$$

Then

(*i*) $\hat{\alpha}(\tilde{\boldsymbol{a}}, \boldsymbol{r}^{\mathrm{c}})^2 \geqslant t^*$;
(*ii*) *Problem* (38) *is a quasiconvex programming problem.*

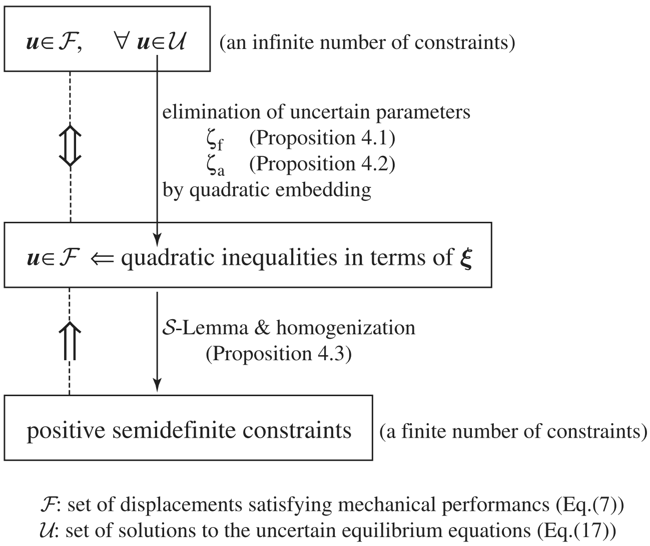

Fig. 3. Reduction of infinitely many constraints into a finite number of positive semidefinite constraints.

Proof. (i) Recall that the robustness function $\hat{\alpha}$ is defined by (25) with Problem (24). It follows from Proposition 4.3 that the constraints of Problem (24) are satisfied if the constraints of Problem (38) are satisfied, which completes the proof.

(ii) Observe that we can reformulate the standard form of quasiconvex optimization problem (3) into the following problem in variables $(t,\boldsymbol{x}) \in \mathbf{R} \times \mathbf{R}^n$:

$$\left.\begin{array}{ll} \min & s, \\ \text{s.t.} & \boldsymbol{x} \in \mathscr{L}_{f_0}(s), \\ & f_i(\boldsymbol{x}) \leqslant 0, \quad i = 1, \ldots, m, \\ & \boldsymbol{A}\boldsymbol{x} = \boldsymbol{b}, \end{array}\right\} \tag{39}$$

where the s-sublevel set $\mathscr{L}_{f_0}(s)$ of f_0 is convex for any $s \in \mathbf{R}$. For a given t and for each $l = 1, \ldots, n^{\mathrm{c}}$, define a set $\mathscr{T}_l$ by

$$\mathscr{T}_l(-t) = \left\{ (\rho_l, \tau_{1l}, \ldots, \tau_{n_{\mathrm{a}}^{\mathrm{m}} l}) \in \mathbf{R}^{n_{\mathrm{a}}^{\mathrm{m}}+1} \,\middle|\, \boldsymbol{H}'_l - \rho_l \boldsymbol{\Omega}_{\mathrm{f}}(t) - \sum_{i=1}^{n_{\mathrm{a}}^{\mathrm{m}}} \tau_{il} \boldsymbol{\Omega}_{\mathrm{a}i}(t) \succeq \boldsymbol{O},\ \rho_l \geqslant 0,\ \tau_{1l}, \ldots, \tau_{n_{\mathrm{a}}^{\mathrm{m}} l} \geqslant 0 \right\}.$$

We easily see that $\mathscr{T}_l(t)$ is convex for any given $t \in \mathbf{R}$, since $\mathscr{T}_l$ is defined by a linear matrix inequality. By regarding $t \in \mathbf{R}$ as an auxiliary variable, we can rewrite Problem (38) as

$$\left.\begin{array}{ll} \max & t, \\ \text{s.t.} & (\rho_l, \tau_{1l}, \ldots, \tau_{n_{\mathrm{a}}^{\mathrm{m}} l}) \in \mathscr{T}_l(-t), \quad l = 1, \ldots, n^{\mathrm{c}}. \end{array}\right\} \tag{40}$$

By putting $t' = -t$, Problem (40) is reduced to

$$\left.\begin{array}{ll} \min & t', \\ \text{s.t.} & (\rho_l, \tau_{1l}, \ldots, \tau_{n_{\mathrm{a}}^{\mathrm{m}} l}) \in \mathscr{T}_l(t'), \quad l = 1, \ldots, n^{\mathrm{c}}. \end{array}\right\} \tag{41}$$

We can embed Problem (41) into Problem (39), i.e., Problem (41) is shown to be a quasiconvex optimization problem, which completes the proof. □

Remark 4.5. The assumption of separable uncertainty is unnecessary in order to obtain a result similar to Lemma 4.4, i.e., to formulate a quasiconvex optimization problem similar to (38) providing a lower bound of $\hat{\alpha}(\tilde{\boldsymbol{a}}, \boldsymbol{r}^{\mathrm{c}})^2$. In (a)–(d) below, we introduce a framework that can represent a broader class of uncertainty models, and briefly show the outline of constructing a corresponding quasiconvex optimization problem. □

(a) Definition of the uncertainty model: let $\boldsymbol{\Theta}_p \in \mathbf{R}^{m_p \times n^{\mathrm{d}}}$, $p = 1, \ldots, q$, denote constant matrices, where $m_p \in \{1, \ldots, n^{\mathrm{d}}\}$. Define $\overline{\mathscr{Z}}_{\mathrm{f}} : \mathbf{R}_+ \mapsto \mathscr{P}(\mathbf{R}^{n^{\mathrm{d}}})$ by

$$\overline{\mathscr{Z}}_{\mathrm{f}}(\alpha) = \left\{ \boldsymbol{\zeta} \in \mathbf{R}^{n^{\mathrm{d}}} \mid \alpha \geqslant \|\boldsymbol{\Theta}_p \boldsymbol{\zeta}\|_2,\ p = 1, \ldots, q \right\}.$$

Here, we have to choose $\boldsymbol{\Theta}_p$ so that $\overline{\mathscr{Z}}_{\mathrm{f}}(\alpha)$ becomes a bounded set for any $\alpha \geqslant 0$. Various uncertainty models can be described by choosing $\boldsymbol{\Theta}_p$ appropriately. Putting $n_{\mathrm{a}}^{\mathrm{m}} = n^{\mathrm{m}}$ in (18), consider the following uncertainty model:

$$a_i = \tilde{a}_i + a_i^0 \zeta_{\mathrm{a}i}, \quad i = 1, \ldots, n^{\mathrm{m}}, \qquad \boldsymbol{\zeta}_{\mathrm{a}} \in \mathscr{Z}_{\mathrm{a}}(\alpha), \tag{42}$$

$$\boldsymbol{f} = \tilde{\boldsymbol{f}} + f^0 \boldsymbol{\zeta}_{\mathrm{f}}, \quad \boldsymbol{\zeta}_{\mathrm{f}} \in \overline{\mathscr{Z}}_{\mathrm{f}}(\alpha). \tag{43}$$

By introducing auxiliary variables $\boldsymbol{\eta} \in \mathbf{R}^{n^{\mathrm{d}}}$ and using (42) and (43), the system (6) of equilibrium equations is reduced to

$$\widetilde{\boldsymbol{K}}\boldsymbol{u} + \sum_{i=1}^{n^{\mathrm{m}}} a_i^0 \zeta_{\mathrm{a}i} \boldsymbol{K}_i \boldsymbol{u} = \boldsymbol{\eta}, \quad \zeta_{\mathrm{a}} \in \mathscr{Z}_{\mathrm{a}}(\alpha), \tag{44}$$

$$\tilde{\boldsymbol{f}} + f^0 \zeta_{\mathrm{f}} = \boldsymbol{\eta}, \quad \zeta_{\mathrm{f}} \in \overline{\mathscr{Z}}_{\mathrm{f}}(\alpha). \tag{45}$$

It should be emphasized that the uncertainty model defined by (42) and (43) does no longer require that the system (6) of equilibrium equations can be decomposed into two parts as (16) and (17). Clearly, the separable uncertainty model introduced in Section 3.2 is included as a particular case of (42) and (43). Moreover, $\overline{\mathscr{Z}}_{\mathrm{f}}$ itself is an extension of $\mathscr{Z}_{\mathrm{f}}$ defined by (19), i.e., $\mathscr{Z}_{\mathrm{f}}$ can be expressed in the form of $\overline{\mathscr{Z}}_{\mathrm{f}}$ by letting $q = 1$ and $\boldsymbol{\Theta}_1$ be an identity matrix. The interval uncertainty set (20) introduced in Remark 3.3 is also included in $\overline{\mathscr{Z}}_{\mathrm{f}}$ as the particular case where $\boldsymbol{\Theta}_p = (\Theta_{pj}) \in \mathbf{R}^{1\times n^{\mathrm{d}}}$, $p = 1, \dots, q$, are the row vectors defined as

$$\Theta_{pj} = \begin{cases} 1 & \text{for } j = p, \\ 0 & \text{for } j \neq p, \end{cases}$$

and $q = n^{\mathrm{d}}$.

(b) Reduction of (45) (analogous to Proposition 4.1): we easily see that (45) can be embedded into the following quadratic inequalities in terms of $\boldsymbol{\eta}$:

$$(f^0\alpha)^2 \geqslant (\boldsymbol{\eta} - \tilde{\boldsymbol{f}})^{\top} \boldsymbol{\Theta}_p^{\top} \boldsymbol{\Theta}_p (\boldsymbol{\eta} - \tilde{\boldsymbol{f}}), \quad p = 1, \dots, q. \tag{46}$$

For consistency with the formulations below, defining $\overline{\boldsymbol{\xi}} \in \mathbf{R}^{n^{\mathrm{n}}+2n^{\mathrm{d}}+1}$ and $\overline{\boldsymbol{\Omega}}_{\mathrm{f}p} \in \mathscr{S}^{n^{\mathrm{n}}+2n^{\mathrm{d}}+1}$, $p = 1, \dots, q$, as

$$\overline{\boldsymbol{\xi}} = (\boldsymbol{v}, \boldsymbol{\eta}, \boldsymbol{u}, 1),$$

$$\overline{\boldsymbol{\Omega}}_{\mathrm{f}p}(\alpha^2) = \begin{pmatrix} \boldsymbol{O} & \boldsymbol{O} & \boldsymbol{O} & \boldsymbol{0} \\ \boldsymbol{O} & -\boldsymbol{\Theta}_p^{\top}\boldsymbol{\Theta}_p & \boldsymbol{O} & \boldsymbol{\Theta}_p^{\top}\boldsymbol{\Theta}_p\tilde{\boldsymbol{f}} \\ \boldsymbol{O} & \boldsymbol{O} & \boldsymbol{O} & \boldsymbol{0} \\ \boldsymbol{0}^{\top} & \tilde{\boldsymbol{f}}^{\top}\boldsymbol{\Theta}_p^{\top}\boldsymbol{\Theta}_p & \boldsymbol{0}^{\top} & (f^0)^2\alpha^2 - \tilde{\boldsymbol{f}}^{\top}\boldsymbol{\Theta}_p^{\top}\boldsymbol{\Theta}_p\tilde{\boldsymbol{f}} \end{pmatrix},$$

we rewrite (46) as

$$\overline{\boldsymbol{\xi}}^{\top} \overline{\boldsymbol{\Omega}}_{\mathrm{f}p} \overline{\boldsymbol{\xi}} \geqslant 0, \quad p = 1, \dots, q,$$

which has been shown to be equivalent to (45).

(c) Reduction of (44) (analogous to Proposition 4.2): by introducing $\boldsymbol{w} \in \mathbf{R}^{n^{\mathrm{m}}}$, we see that (44) is equivalently rewritten as

$$\boldsymbol{\Psi}\boldsymbol{w} = \widetilde{\boldsymbol{K}}\boldsymbol{u} - \boldsymbol{\eta}, \quad (31). \tag{47}$$

By using quadratic embedding and eliminating $\boldsymbol{w}$, we see that (47) is equivalent to

$$(a_i^0\alpha)^2(\boldsymbol{b}_i^{\top}\boldsymbol{u})^2 - \left[\boldsymbol{\Psi}_{i,\cdot}^{\dagger}(\widetilde{\boldsymbol{K}}\boldsymbol{u} - \boldsymbol{\eta}) + \boldsymbol{\Psi}^{\perp}\boldsymbol{v}\right]^2 \geqslant 0, \quad i = 1, \dots, n^{\mathrm{m}}.$$

Thus, the condition (44) is embedded into the following series of quadratic inequalities:

$$\overline{\boldsymbol{\xi}}^{\top} \overline{\boldsymbol{\Omega}}_{\mathrm{a}i}(\alpha^2) \overline{\boldsymbol{\xi}} \geqslant 0, \quad i = 1, \dots, n^{\mathrm{m}},$$

where $\overline{\boldsymbol{\Omega}}_{\mathrm{a}i}(\alpha^2) \in \mathcal{S}^{n^{\mathrm{n}}+2n^{\mathrm{d}}+1}$, $i = 1, \dots, n^{\mathrm{m}}$, are defined as

$$\overline{\boldsymbol{\Omega}}_{\mathrm{a}i}(\alpha^2) = \alpha^2 \begin{pmatrix} \boldsymbol{O} & \boldsymbol{O} & \boldsymbol{O} & \boldsymbol{0} \\ \boldsymbol{O} & \boldsymbol{O} & \boldsymbol{O} & \boldsymbol{0} \\ \boldsymbol{O} & \boldsymbol{O} & (a_i^0)^2 \boldsymbol{b}_i \boldsymbol{b}_i^\top & \boldsymbol{0} \\ \boldsymbol{0}^\top & \boldsymbol{0}^\top & \boldsymbol{0}^\top & 0 \end{pmatrix} + \begin{pmatrix} -(\boldsymbol{\Psi}^\perp_{i,\cdot})^\top \boldsymbol{\Psi}^\perp_{i,\cdot} & (\boldsymbol{\Psi}^\perp_{i,\cdot})^\top \boldsymbol{\Psi}^\dagger_{i,\cdot} & -(\boldsymbol{\Psi}^\perp_{i,\cdot})^\top \boldsymbol{\Psi}^\dagger_{i,\cdot} \widetilde{\boldsymbol{K}} & \boldsymbol{0} \\ (\boldsymbol{\Psi}^\dagger_{i,\cdot})^\top \boldsymbol{\Psi}^\perp_{i,\cdot} & -(\boldsymbol{\Psi}^\dagger_{i,\cdot})^\top \boldsymbol{\Psi}^\dagger_{i,\cdot} & (\boldsymbol{\Psi}^\dagger_{i,\cdot})^\top \boldsymbol{\Psi}^\dagger_{i,\cdot} \widetilde{\boldsymbol{K}} & \boldsymbol{0} \\ -(\boldsymbol{\Psi}^\dagger_{i,\cdot} \widetilde{\boldsymbol{K}})^\top \boldsymbol{\Psi}^\perp_{i,\cdot} & (\boldsymbol{\Psi}^\dagger_{i,\cdot} \widetilde{\boldsymbol{K}})^\top \boldsymbol{\Psi}^\dagger_{i,\cdot} & -(\boldsymbol{\Psi}^\dagger_{i,\cdot} \widetilde{\boldsymbol{K}})^\top (\boldsymbol{\Psi}^\dagger_{i,\cdot} \widetilde{\boldsymbol{K}}) & \boldsymbol{0} \\ \boldsymbol{0}^\top & \boldsymbol{0}^\top & \boldsymbol{0}^\top & 0 \end{pmatrix}.$$

(d) Resulting problem (corresponding to Lemma 4.4): it is easy to obtain a result similar to Proposition 4.3. Consider the following problem in variables $(t, \boldsymbol{\rho}, \boldsymbol{\tau}) \in \mathbf{R} \times \mathbf{R}^{qn^{\mathrm{c}}} \times \mathbf{R}^{n^{\mathrm{m}} n^{\mathrm{c}}}$ with $\boldsymbol{\rho} = (\rho_{11}, \dots, \rho_{q1}, \dots, \rho_{1n^{\mathrm{c}}}, \dots, \rho_{qn^{\mathrm{c}}})$ and $\boldsymbol{\tau} = (\tau_{11}, \dots, \tau_{n^{\mathrm{m}}1}, \dots, \tau_{1n^{\mathrm{c}}}, \dots, \tau_{n^{\mathrm{m}}n^{\mathrm{c}}})$:

$$t^* := \max \left\{ t : \boldsymbol{H}'_l - \sum_{p=1}^{q} \rho_{pl} \overline{\boldsymbol{\Omega}}_{\mathrm{f}p}(t) - \sum_{i=1}^{n^{\mathrm{m}}} \tau_{il} \overline{\boldsymbol{\Omega}}_{\mathrm{a}i}(t) \succeq \boldsymbol{O},\ l = 1, \dots, n^{\mathrm{c}},\ \ \boldsymbol{\rho} \geqslant \boldsymbol{0},\ \boldsymbol{\tau} \geqslant \boldsymbol{0} \right\}. \tag{48}$$

Then (i) $\hat{\alpha}(\tilde{\boldsymbol{a}}, \boldsymbol{r}^{\mathrm{c}})^2 \geqslant t^*$; (ii) Problem (48) is a quasiconvex programming problem. □

Lemma 4.4(ii) is important, since it guarantees that Problem (38) can be solved by using a bisection method (Boyd and Vandenberghe, 2004, Section 4.2.5). Let $\boldsymbol{I}$ denote the identity matrix with an appropriate size. For a fixed t, consider the following problem in variables $(s, \boldsymbol{\rho}, \boldsymbol{\tau}) \in \mathbf{R} \times \mathbf{R}^{n^{\mathrm{c}}} \times \mathbf{R}^{n^{\mathrm{m}}_{\mathrm{a}} n^{\mathrm{c}}}$:

$$\left. \begin{array}{ll} \min & s, \\ \text{s.t.} & \boldsymbol{H}'_l - \rho_l \boldsymbol{\Omega}_{\mathrm{f}}(t) - \sum_{i=1}^{n^{\mathrm{m}}_{\mathrm{a}}} \tau_{il} \boldsymbol{\Omega}_{\mathrm{a}i}(t) + s\boldsymbol{I} \succeq \boldsymbol{O}, \\ & \rho_l \geqslant 0, \quad \tau_{1l}, \dots, \tau_{n^{\mathrm{m}}_{\mathrm{a}} l} \geqslant 0, \qquad l = 1, \dots, n^{\mathrm{c}}, \end{array} \right\} \tag{49}$$

which is regarded as a convex feasibility problem of Problem (38) (Boyd and Vandenberghe, 2004, Section 4.2.5). Note that Problem (49) is an SDP problem, which can be embedded into the dual standard form (2). Let $(s^*, \boldsymbol{\rho}^*, \boldsymbol{\tau}^*)$ denote an optimal solution to Problem (49) for a given t. Recall that t^* has been defined in (38). If $s^* \leqslant 0$, then $(t, \boldsymbol{\rho}^*, \boldsymbol{\tau}^*)$ is a feasible solution of Problem (38), which implies $t^* \geqslant t$. On the contrary, if $s^* > 0$, then $t^* < t$. Consequently, we see that the following bisection method solves Problem (38):

Algorithm 4.6 (*Bisection method for Problem* (38))

Step 0: Choose $\underline{t}^0$ and $\overline{t}^0$ satisfying $0 \leqslant \underline{t}^0 \leqslant t^* \leqslant \overline{t}^0$, and the tolerance $\epsilon > 0$. Set $k := 0$.
Step 1: If $\overline{t}^k - \underline{t}^k \leqslant \epsilon$, then STOP. Otherwise, set $t := (\underline{t}^k + \overline{t}^k)/2$.
Step 2: Find an optimal solution $(s^*, \boldsymbol{\rho}^*, \boldsymbol{\tau}^*)$ to the SDP problem (49).
Step 3: If $s^* \leqslant 0$, then set $\underline{t}^{k+1} := t$ and $\overline{t}^{k+1} := \overline{t}^k$. Otherwise, set $\overline{t}^{k+1} := t$ and $\underline{t}^{k+1} := \underline{t}^k$.
Step 4: Set $k := k + 1$, and go to Step 1.

Algorithm 4.6 finds a global optimal solution to Problem (38) by solving some SDP problems, where exactly $\lceil \log_2((\overline{t}^0 - \underline{t}^0)/\epsilon) \rceil$ iterations are required before the algorithm terminates. Here, for $p \in \mathbf{R}$, $\lceil p \rceil$ denotes the minimum integer that is not smaller than p. At Step 0, we may simply choose $\underline{t}^0 = 0$, and a sufficiently large $\overline{t}^0$. As a possible choice of $\overline{t}^0$, we may compute the robustness function in the case where the vector of member cross-sectional areas $\boldsymbol{a}$ is certain, and only $\boldsymbol{f}_{\mathrm{f}}$ has uncertainty without changing the settings in (17). Since this situation can be regarded as a restricted case of the perturbation defined by (16) and (17), the square of the robustness function with the certain $a_1, \dots, a_{n^{\mathrm{m}}_{\mathrm{a}}}$ corresponds to an upper bound of t^* with the uncertain $a_1, \dots, a_{n^{\mathrm{m}}_{\mathrm{a}}}$. It should be emphasized that, by using Proposition 5.1 in (Kanno and Takewaki, 2004a), the exact value of the robustness function can be computed easily if all the member cross-sectional areas are certain. If t^* is not bounded from above, then we cannot choose $\bar{t}^0$ satisfying the condition in Step 0. In this case, Algorithm 4.6 terminates with $t = \bar{t}^k$ for any positive (finite) $\bar{t}^0$. The positive infinite robustness function implies that the uncertainty considered is not critical for the truss in the sense of mechanical performance constraints (10). Hence, from a practical point of view, it suffices to know that t^* is very large, even if no guarantee is obtained for t^* and/or $\hat{\alpha}(\tilde{\boldsymbol{a}}, \boldsymbol{r}^{\rm c})$ to be positive infinite.

At Step 2 of each iteration, we solve Problem (49), which can be embedded into the dual SDP problem (2) with $m = n^{\rm c}(n_{\rm a}^{\rm m} + 1) + 1$ and $n = n^{\rm c}(n^{\rm n} + n^{\rm d} + n_{\rm a}^{\rm m} + 2)$. It should be emphasized that a global optimal solution to an SDP problem (49) can be obtained by using the primal–dual interior-point method, where the number of arithmetic operations is bounded by a polynomial of m and n (Kojima et al., 1997; Wolkowicz et al., 2000). This indicates that the computational cost required by Algorithm 4.6 does not increase drastically even for large scale trusses.

Remark 4.7. Recall that we have introduced a framework of uncertainty representation in (42) and (43) of Remark 4.5. It has been illustrated that this framework can express a broader class of uncertainty models including the separable uncertainty defined in Section 3. Then we have attained the quasiconvex problem (48) providing a lower bound on the robustness function. In a manner similar to Algorithm 4.6, we can obtain the optimal solution of Problem (48) by using the bisection method in which we solve some convex feasibility problems formulated as the SDP problems. Note that Problem (48) has a slightly different form than Problem (38). Hence, the resulting SDP problem will be different from Problem (49). Since the uncertainty representation (42) and (43) includes the separable uncertainty model, we can obtain a lower bound of the robustness function of a truss with the separable uncertainty by solving Problem (48). However, it is desirable to solve Problem (38) rather than Problem (48) if a truss obeys the separable uncertainty model. In what follows, we investigate the size of SDP problems solved in the bisection method for Problems (38) and (48), i.e., we compare m and n when the corresponding feasibility problems are transformed into the dual standard form (2).

(a) Consider the separable uncertainty model. Then the optimal solution of Problem (38) is obtained by solving Problem (49) successively. Here, Problem (49) has the $n^{\rm c}(n_{\rm a}^{\rm m} + q)$ linear inequality constraints and requirement such that $n^{\rm c}$ symmetric matrices in $\mathcal{S}^{n^{\rm n}+n^{\rm d}+1}$ should be positive semidefinite, i.e., Problem (49) is embedded into the form of Problem (2) with $n = n^{\rm c}(n^{\rm n} + n^{\rm d} + n_{\rm a}^{\rm m} + q + 1)$. On the other hand, the convex feasibility problem for Problem (48) has the $n^{\rm c}(n_{\rm a}^{\rm m} + q)$ linear inequality constraints and requirement such that $n^{\rm c}$ symmetric matrices in $\mathcal{S}^{n^{\rm n}+2n^{\rm d}+1}$ should be positive semidefinite, i.e., $n = n^{\rm c}(n^{\rm n} + 2n^{\rm d} + n_{\rm a}^{\rm m} + q + 1)$ in the form of Problem (2). In both cases, we see $m = n^{\rm c}(n_{\rm a}^{\rm m} + q) + 1$. Thus, if the truss obeys the separable uncertainty model, then it is recommended to use the formulation (38) rather than (48) from the view point of problem size n.

(b) It should be also noted that m and n depend on the definition of the load uncertainty set $\overline{\mathscr{Z}}_{\rm f}$ in Remark 4.5, since they depend on q. Consider the uncertainty set defined in (42) and (43). Then the convex feasibility problem for Problem (48) is transformed into the form of Problem (2) with $m = n^{\rm c}(n^{\rm m} + q) + 1$ and $n = n^{\rm c}(n^{\rm n} + 2n^{\rm d} + n^{\rm m} + q + 1)$. As observed in Remark 4.5, we see $q = 1$ if we define $\overline{\mathscr{Z}}_{\rm f}$ by using the l_2-norm as is done in (19). On the other hand, we see $q = n^{\rm d}$ if we use the l_∞-norm as is done in (20). Consequently, using (19) has less numerical complexity compared with (20) in the sense of m and n. □

5. Numerical experiments

The lower bounds on the robustness functions are computed for various trusses by using Algorithm 4.6. In Step 2 in Algorithm 4.6, the SDP problem (49) is solved by using SeDuMi Ver. 1.05 (Sturm, 1999), which implements the primal–dual interior-point method for the linear programming problems over symmetric cones. Computation has been carried out on Pentium M (1.5 GHz with 1 GB memory) with MATLAB Ver. 6.5.1 (The MathWorks, 2002).

5.1. Three-bar truss

Recall the three-bar truss introduced in Example 3.2 and is illustrated in Fig. 1. Nodes (a) and (b) are pin-supported at $(x, y) = (0, 0)$ and $(100, 0)$ in cm, respectively. The location of node (c) in the direction of the x-axis is constrained at $x = 100$ in cm. The lengths of members (1), (2), and (3), respectively, are 50.0 cm, $100\sqrt{2}$ cm, and 50.0 cm. The elastic modulus is 200 GPa.

We assume that the cross-sectional area of member (1) has uncertainty, whereas those of members (2) and (3) are certain. The external loads applied at node (d) have uncertainty, whereas those applied at node (c) are certain. The nominal cross-sectional areas are given as

$$\tilde{\boldsymbol{a}} = (30.0, 50.0, 20.0)\ \text{cm}^2.$$

We consider the following two nominal load scenarios:

$$\text{(Case 1)}: \quad \tilde{f}_{\text{a}} = 700\ \text{kN}, \quad \tilde{\boldsymbol{f}}_{\text{f}} = (0, 1000)\ \text{kN};$$
$$\text{(Case 2)}: \quad \tilde{f}_{\text{a}} = 300\ \text{kN}, \quad \tilde{\boldsymbol{f}}_{\text{f}} = (0, 1300)\ \text{kN}.$$

The coefficients of uncertainty in (16) and (17) are

$$a_1^0 = 1.0\ \text{cm}^2, \quad f^0 = 100.0\ \text{kN}.$$

We denote by σ_i the stress of the ith member. Consider the stress constraints of all members formulated as

$$|\sigma_i| \leqslant \sigma_i^{\text{c}}, \quad i = 1, \ldots, n^{\text{m}}, \tag{50}$$

where $\sigma_i^{\text{c}} = 1.0$ GPa, $i = 1, \ldots, n^{\text{m}}$.

The lower bounds of the robustness functions $\hat{\alpha}(\tilde{\boldsymbol{a}}, \boldsymbol{\sigma}^{\text{c}})$ are computed by using Algorithm 4.6 for the two cases. We set $\underline{t}^0 = 0$, $\overline{t}^0 = 100.0$, and $\epsilon = 10^{-3}$. The lower bounds $(t^*)^{1/2}$ are obtained as 5.3847 and 4.9498 for (Case 1) and (Case 2), respectively, where 17 iterations are required in the algorithm for each case. In this example, n^{n} defined by (27) is $n^{\text{n}} = 0$. Hence, the dimensions of SDP problem in a standard form (2) are $n = 18$ and $m = 7$, respectively. The average and standard deviation of CPU time, respectively, required to solve each SDP problem (49) are 0.31 s and 0.10 s.

In order to verify these results, we randomly generate a number of ζ_{a} and ζ_{f} satisfying (18) and (19), respectively, by putting $\alpha = (t^*)^{1/2}$, and compute the corresponding member stresses σ_i. Figs. 4 and 5 show the obtained stress states $(\sigma_1/\sigma_1^{\text{c}}, \sigma_3/\sigma_3^{\text{c}})$ for (Case 1) and (Case 2), respectively. It is observed from Figs. 4 and 5 that the stress constraints (50) for members (1) and (3) are satisfied for all generated $(\zeta_{\text{a}}, \zeta_{\text{f}})$. σ_2 also satisfies (50) for all generated $(\zeta_{\text{a}}, \zeta_{\text{f}})$, where $|\sigma_2|$ is always strictly smaller than σ_2^{c}. Consequently, the obtained values $(t^*)^{1/2}$ are verified to be conservative estimations, or lower bounds, of $\hat{\alpha}$. In (Case 1), it is observed from Fig. 4 that the worst case corresponds to $(\zeta_{\text{a}}, \zeta_{\text{f}})$ such that the constraint $\sigma_1 \leqslant \sigma_1^{\text{c}}$ becomes active. On the other hand, in (Case 2), we see from Fig. 5 that the constraint $\sigma_3 \leqslant \sigma_3^{\text{c}}$ becomes active at the worst case. Thus, the worst case depends on the settings of nominal values of external loads. In Figs. 4 and 5, we see that the maximum values of σ_1 and σ_3 are very close to σ_1^{c} and σ_3^{c}, respectively. This implies that the obtained values $(t^*)^{1/2}$ are sufficiently tight lower bounds, i.e., $(t^*)^{1/2}$ are very close to the exact $\hat{\alpha}$.

5.2. 20-bar truss

Consider a plane truss illustrated in Fig. 6, where $n^{\text{d}} = 16$ and $n^{\text{m}} = 20$. Nodes (a) and (b) are pin-supported at $(x, y) = (0, 0)$ and $(0, 100)$ in cm, respectively. The lengths of members in the x- and y-directions, respectively, are 100 cm and 50 cm. The elastic modulus of each member is 200 GPa.

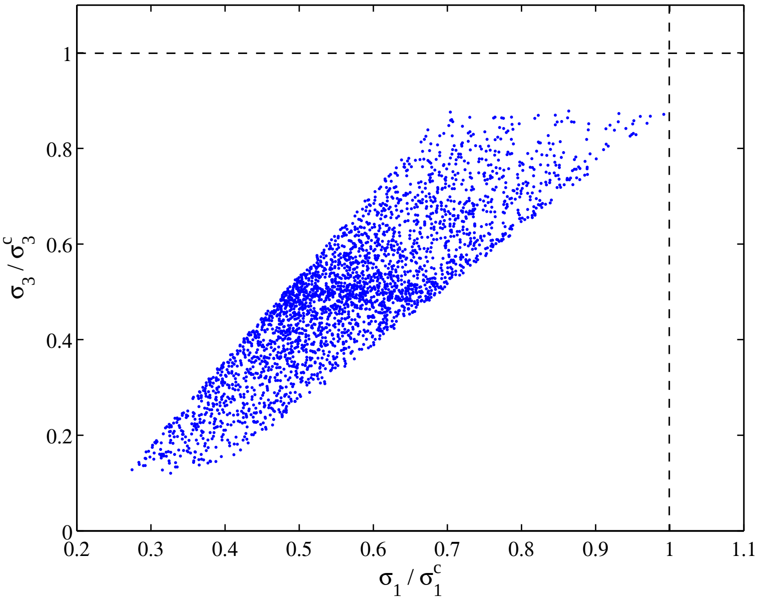

Fig. 4. Stress states of the 3-bar truss (Case 1) for randomly generated $\zeta_a \in \mathscr{Z}_a(\alpha)$ and $\zeta_f \in \mathscr{Z}_f(\alpha)$ with $\alpha = 5.3847$.

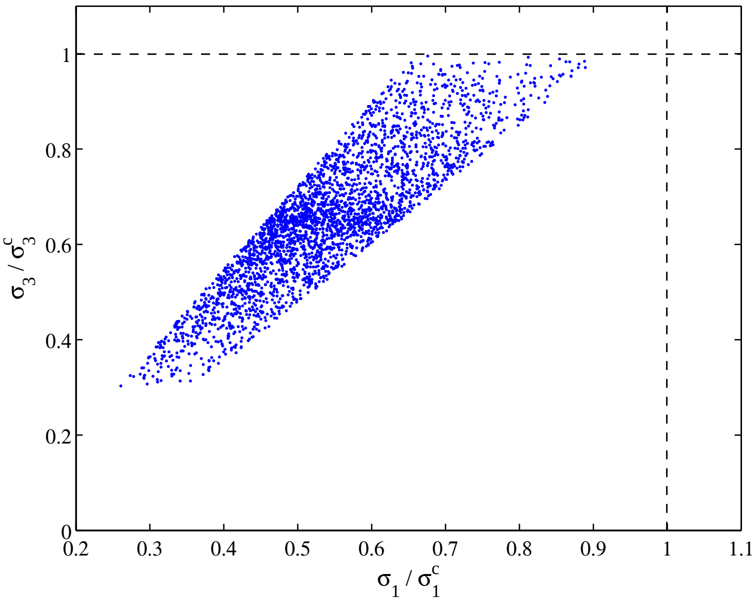

Fig. 5. Stress states of the 3-bar truss (Case 2) for randomly generated $\zeta_a \in \mathscr{Z}_a(\alpha)$ and $\zeta_f \in \mathscr{Z}_f(\alpha)$ with $\alpha = 4.9498$.

We assume that the cross-sectional area of members (1)–(5) have uncertainty, whereas those of members (6)–(20) are certain. The external loads applied at nodes (e)–(j) have uncertainty, whereas those applied at nodes (c) and (d) are certain, i.e., $n_a^m = 5$, $n_a^d = 4$, and $n_f^d = 12$. No external loads are applied at nodes (c) and (d), i.e., $\tilde{\boldsymbol{f}}_a = \boldsymbol{0}$. The nominal external loads (200.0, 0) kN, (500.0, 0) kN, (700.0, −100.0) kN, and

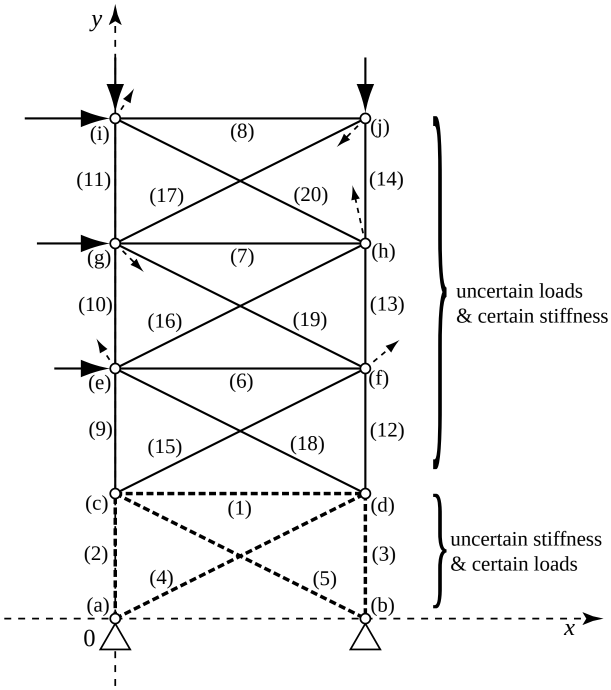

Fig. 6. 20-bar truss.

$(0, -100.0)$ kN, respectively, are applied at nodes (e), (g), (i), and (j). As the sets of nominal cross-sectional areas, we consider the following three cases:

$$\text{(Case 1)}: \ \tilde{a}_i = 26.0 \text{ cm}^2, \quad i = 1, \ldots, 5;$$
$$\text{(Case 2)}: \ \tilde{a}_i = 30.0 \text{ cm}^2, \quad i = 1, \ldots, 5;$$
$$\text{(Case 3)}: \ \tilde{a}_i = 34.0 \text{ cm}^2, \quad i = 1, \ldots, 5;$$

and

$$\tilde{a}_i = 20.0 \text{ cm}^2, \quad i = 6, \ldots, 20.$$

The coefficients of uncertainty in (16) and (17) are

$$a_i^0 = 1.0 \text{ cm}^2, \quad i = 1, \ldots, 5,$$
$$f^0 = 100.0 \text{ kN}.$$

We consider the stress constraints (50) for all members with $\sigma_i^{\mathrm{c}} = 1.0$ GPa, $i = 1, \ldots, n^{\mathrm{m}}$.

The lower bound of the robustness function $\hat{\alpha}(\tilde{\boldsymbol{a}}, \boldsymbol{\sigma}^{\mathrm{c}})$ is computed by using Algorithm 4.6 for each case. We set $\underline{t}^0 = 0$, $\bar{t}^0 = 50.0$, and $\epsilon = 10^{-3}$. The lower bounds $(t^*)^{1/2}$ are obtained as 1.2679, 2.1243, and 2.1645 for (Case 1), (Case 2), and (Case 3), respectively, where 16 iterations are required in the algorithm for each case. Thus, the robustness functions depends on the nominal cross-sectional areas. Note that $n^{\mathrm{n}} = 1$ in this example, where n^{n} has been defined in (27). Hence, if we embed the SDP problem (49) into a dual standard form (2), the dimensions of the resulting problem are $n = 480$ and $m = 121$. The average and standard deviation of CPU time, respectively, required to solve each SDP problem (49) are 7.08 s and 1.64 s.

We next randomly generate a number of ζ_{a} and ζ_{f} satisfying (18) and (19), respectively, by putting $\alpha = (t^*)^{1/2}$, and compute the corresponding member stresses σ_i. Figs. 7–9 show the obtained member

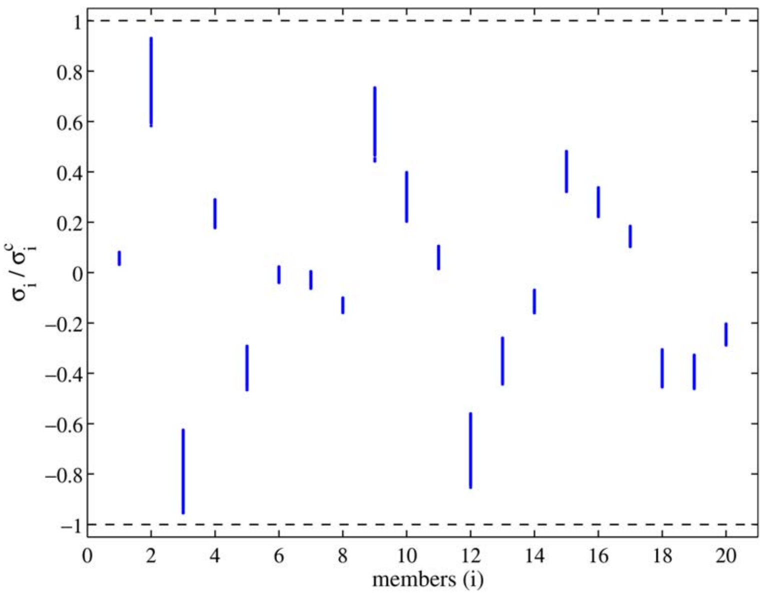

Fig. 7. Stress states of the 20-bar truss (Case 1) for randomly generated $\zeta_{\mathrm{a}} \in \mathscr{Z}_{\mathrm{a}}(\alpha)$ and $\zeta_{\mathrm{f}} \in \mathscr{Z}_{\mathrm{f}}(\alpha)$ with $\alpha = 1.2679$.

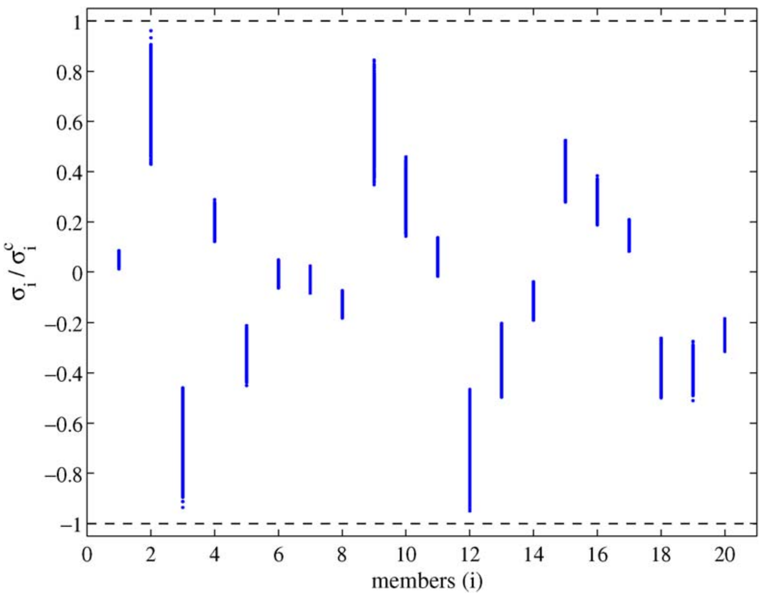

Fig. 8. Stress states of the 20-bar truss (Case 2) for randomly generated $\zeta_{\mathrm{a}} \in \mathscr{Z}_{\mathrm{a}}(\alpha)$ and $\zeta_{\mathrm{f}} \in \mathscr{Z}_{\mathrm{f}}(\alpha)$ with $\alpha = 2.1243$.

stresses $\sigma_i/\sigma_i^{\mathrm{c}}$, $i = 1, \ldots, 20$, for (Case 1), (Case 2), and (Case 3), respectively. It is observed from Figs. 7–9 that the stress constraints (50) for all members are satisfied for all generated $(\zeta_{\mathrm{a}}, \zeta_{\mathrm{f}})$, which verifies that the obtained values $(t^*)^{1/2}$ are certainly lower bounds of $\hat{\alpha}$. In (Case 1), it is observed from Fig. 7 that the worst case corresponds to $(\zeta_{\mathrm{a}}, \zeta_{\mathrm{f}})$ such that the constraints $\sigma_2 \leqslant \sigma_2^{\mathrm{c}}$ and/or $\sigma_3 \geqslant -\sigma_3^{\mathrm{c}}$ become active. In (Case 3),

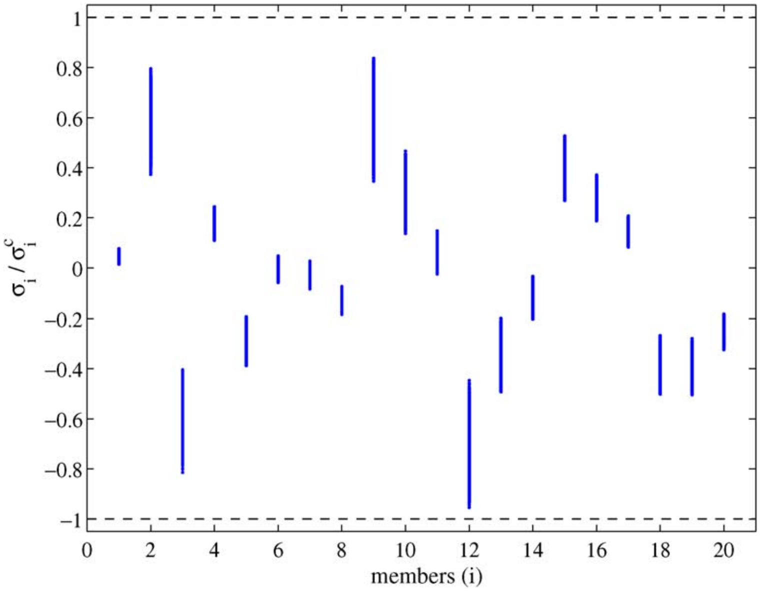

Fig. 9. Stress states of the 20-bar truss (Case 3) for randomly generated $\zeta_a \in \mathscr{Z}_a(\alpha)$ and $\zeta_f \in \mathscr{Z}_f(\alpha)$ with $\alpha = 2.1645$.

from Fig. 9, we can see that the worst case corresponds to (ζ_a, ζ_f) such that the constraints $\sigma_{12} \geqslant -\sigma_{12}^c$ becomes active. On the contrary, in (Case 2), we see from Fig. 8 that all the constraints $\sigma_2 \leqslant \sigma_2^c$, $\sigma_3 \geqslant -\sigma_3^c$, and $\sigma_{12} \geqslant -\sigma_{12}^c$ may possibly become active. Thus, the critical members, the stress constraints of which possibly become active, depend on the settings of nominal values of member cross-sectional areas. It is observed from Figs. 7–9 that, for each case, there exists at least one member whose magnitude of stress σ_i possibly becomes very close to its upper bound σ_i^c. This implies that Algorithm 4.6 provides sufficiently tight lower bounds, i.e., the obtained value $(t^*)^{1/2}$ is very close to the exact value of $\hat{\alpha}$ in each case.

6. Conclusions

In this paper, we have proposed an approximation algorithm for computing the robustness functions of trusses under the load and structural uncertainty models. The effective method for computing lower bounds of the robustness functions may permit us to apply the info-gap decision theory (Ben-Haim, 2001) to designing trusses which never encounter violation of mechanical performance constraints under the uncertainty considered.

We have introduced an uncertainty model referred to as a separable uncertainty model, where the external forces as well as the member stiffness include uncertain parameters. More general framework has been also defined to represent coupled uncertainties of the external forces and the member stiffnesses. We assume that the constraints on mechanical performance can be expressed by using some quadratic inequalities in terms of displacements. In fact, we can deal with the polynomial inequality constraints in terms of displacements by converting them into a finite number of quadratic inequalities. Then the robustness function is obtained as the optimal objective value of a semi-infinite optimization problem having a finite number of variables and infinitely many constraint conditions.

By using quadratic embedding of the uncertainty and the $\mathscr{S}$-procedure, we have formulated some finite-dimensional semidefinite constraints corresponding to a sufficient condition for the infinite number of constraints. Then a quasiconvex optimization problem is formulated, which provides the lower bound, i.e., a conservative estimation, of the robustness function. In order to obtain a global optimal solution of the present quasiconvex optimization problem, a bisection method has been proposed, where a finite number of SDP problems are successively solved by the primal–dual interior-point method.

In the numerical examples, lower bounds on the robustness functions of trusses with separable uncertainties have been computed under various conditions of uncertainties by using the proposed algorithm. It has been shown that the lower bounds of the robustness function, as well as the worst cases, depend on the nominal values of member cross-sectional areas and external forces. We have also illustrated that the obtained lower bounds are very close to the exact values of the robustness function.

Acknowledgements

The authors are grateful to two anonymous referees for many valuable comments to improve the paper. Especially, much of the result in Remark 4.5 is due to suggestions of one of them.

References

Ben-Haim, Y., 2001. Information-gap Decision Theory. Academic Press, London, UK.

Ben-Haim, Y., Elishakoff, I., 1990. Convex Models of Uncertainty in Applied Mechanics. Elsevier, Amsterdam, The Netherlands.

Ben-Tal, A., Nemirovski, A., 1997. Robust truss topology optimization via semidefinite programming. SIAM Journal on Optimization 7, 991–1016.

Ben-Tal, A., Nemirovski, A., 2001. Lectures on Modern Convex Optimization: Analysis, Algorithms, and Engineering Applications. SIAM, Philadelphia, PA.

Ben-Tal, A., Nemirovski, A., 2002. Robust optimization—methodology and applications. Mathematical Programming B 92, 453–480.

Boyd, S., Vandenberghe, L., 2004. Convex Optimization. Cambridge University Press, Cambridge, UK.

Boyd, S., El Ghaoui, L., Feron, E., Balakrishnan, V., 1994. Linear Matrix Inequalities in System and Control Theory. SIAM, Philadelphia, PA.

Calafiore, G., El Ghaoui, L., 2004. Ellipsoidal bounds for uncertain linear equations and dynamical systems. Automatica 40, 773–787.

Choi, K.K., Tu, J., Park, Y.H., 2001. Extensions of design potential concept for reliability-based design optimization to nonsmooth and extreme cases. Structural and Multidisciplinary Optimization 22, 335–350.

Doltsinis, I., Kang, Z., 2004. Robust design of structures using optimization methods. Computer Methods in Applied Mechanics and Engineering 193, 2221–2237.

Kanno, Y., Takewaki, I., 2004a. Direct evaluation of robustness functions of trusses associated with stress constraints. BGE Research Report 04-03, Building Geoenvironment Engineering Laboratory, Kyoto University, Japan.

Kanno, Y., Takewaki, I., 2004b. Sequential semidefinite program for maximum robustness design of structures under load uncertainties. BGE Research Report 04-05, Building Geoenvironment Engineering Laboratory, Kyoto University, Japan.

Kharmanda, G., Olhoff, N., Mohamed, A., Lemaire, M., 2004. Reliability-based topology optimization. Structural and Multidisciplinary Optimization 26, 295–307.

Kojima, M., Tunçel, L., 2000. Cones of matrices and successive convex relaxations of nonconvex sets. SIAM Journal on Optimization 10, 750–778.

Kojima, M., Shindoh, S., Hara, S., 1997. Interior-point methods for the monotone semidefinite linear complementarity problem in symmetric matrices. SIAM Journal on Optimization 7, 86–125.

Muhanna, R.L., Mullen, R.L., 2001. Uncertainty in mechanics problems—Interval-based approach. Journal of Engineering Mechanics (ASCE) 127, 557–566.

Ohsaki, M., Fujisawa, K., Katoh, N., Kanno, Y., 1999. Semi-definite programming for topology optimization of truss under multiple eigenvalue constraints. Computer Methods in Applied Mechanics and Engineering 180, 203–217.

Pantelides, C.P., Ganzerli, S., 1998. Design of trusses under uncertain loads using convex models. Journal of Structural Engineering (ASCE) 124, 318–329.

Sturm, J.F., 1999. Using SeDuMi 1.02, a MATLAB toolbox for optimization over symmetric cones. Optimization Methods and Software 11/12, 625–653.

Takewaki, I., Ben-Haim, Y., in press. Info-gap robust design with load and model uncertainties. Journal of Sound and Vibration.
The MathWorks, Inc., 2002. Using MATLAB. The MathWorks, Inc., Natick, MA.
Tsompanakis, Y., Papadrakakis, M., 2004. Large-scale reliability-based structural optimization. Structural and Multidisciplinary Optimization 26, 429–440.
Wolkowicz, H., Saigal, R., Vandenberghe, L. (Eds.), 2000. Handbook of Semidefinite Programming—Theory, Algorithms, and Applications. Kluwer Academic Publishers, Dordrecht, The Netherlands.